SEPTEMBER 2023

M.Sc. in Civil Engineering

YOUSEF ALHAMMOUDI

REPUBLIC OF TÜRKİYE

GAZİANTEP UNIVERSITY

GRADUATE SCHOOL OF NATURAL & APPLIED SCIENCES

NUMERICAL STUDY OF LOCAL SCOUR AROUND BRIDGE PIER WITH COLLAR USING FLOW-3D SOFTWARE

M.Sc. THESIS

IN

CIVIL ENGINEERING

BY

YOUSEF ALHAMMOUDI

SEPTEMBER 2023

NUMERICAL STUDY OF LOCAL SCOUR AROUND BRIDGE PIER WITH COLLAR USING FLOW-3D SOFTWARE

M.Sc. Thesis

in

Civil Engineering

Gaziantep University

Supervisor

Prof. Dr. Mustafa GÜNAL

By

Yousef ALHAMMOUDI

September 2023

NUMERICAL STUDY OF LOCAL SCOUR AROUND BRIDGE PIER WITH COLLAR USING FLOW-3D SOFTWARE

submitted by **Yousef ALHAMMOUDI** in partial fulfillment of the requirements for the degree of Master of Science in **Civil Engineering, Gaziantep University** is approved by,

Prof. Dr. Çiğdem AYKAÇ
Director of the Graduate School of Natural and Applied Sciences. ..………..............

Prof. Dr. Nildem TAYŞİ
Head of the Department of Civil Engineering ………...............

Prof. Dr. Mustafa GÜNAL
Supervisor, Civil Engineering
Gaziantep University ………...............

Exam Date: 12 September 2023

Examining Committee Members:

Prof. Dr. Mustafa GÜNAL
Gaziantep University ………...............

Prof. Dr. Ali AYTEK
Gaziantep Islam Science and Technology University ………............

Prof. Dr. AYTAÇ GÜVEN
Gaziantep University ………...............

I hereby declare that all information in this document has been obtained and presented in accordance with academic rules and ethical conduct. I also declare that, as required by these rules and conduct, I have fully cited and referenced all material and results that are not original to this work.

Yousef ALHAMMOUDI

ABSTRACT

NUMERICAL STUDY OF THE LOCAL SCOUR AROUND BRIDGE PIER WITH COLLAR USING FLOW-3D SOFTWARE

ALHAMMOUDI, Yousef
M.Sc. in Civil Engineering
Supervisor: Prof. Dr. Mustafa GÜNAL
September 2023
69 pages

The scouring of sediments around bridge foundations in the riverbed leading to collapse remains a significant problem, causing both economic losses and risking human lives. This investigation focuses on studying the effects of collar for reducing scour around bridge piers by using two different types of bridge pier shapes namely circular and nosed pier. In recent years, three-dimensional simulation methods for scouring have gained popularity due to advancements in computer capabilities and software, enabling the widespread utilization of Computational Fluid Dynamics (CFD) to analyze scour phenomena in various industrial and environmental applications. A numerical model is created for bridge pier with collar to compare and validate the results obtained from the experimental study of Ismael A. et al., in 2015. Findings shows that local scour is reduced by using collared bridge pier.

Key Words: Scour, Flow 3D, Circular pier, Nosed pier, Collar

ÖZET

YAKALI KÖPRÜ AYAĞI ÇEVRESİNDE OLUŞAN YEREL OYULMANIN FLOW-3D YAZILIMI KULLANILARAK SAYISAL ÇALIŞMASI

ALHAMMOUDI, Yousef
Yüksek Lisans Tezi, İnşaat Mühendisliği
Danışman: Prof. Dr. Mustafa GÜNAL
Ağustos 2023
69 sayfa

Nehir yatağındaki köprü temellerinin etrafındaki malzemenin aşınarak çökmeye yol açması, hem ekonomik kayıplara neden olan hem de insan hayatını tehlikeye atan önemli bir sorun olmaya devam ediyor. Bu araştırma, dairesel ve burunlu olmak üzere iki farklı köprü ayağı şekli kullanılarak köprü ayakları etrafındaki oyulmanın azaltılmasında yakanın etkilerinin incelenmesine odaklanmaktadır. Son yıllarda, bilgisayar yetenekleri ve yazılımlardaki gelişmeler nedeniyle oyulma için üç boyutlu simülasyon yöntemleri popülerlik kazanmış ve çeşitli endüstriyel ve çevresel uygulamalarda oyulma olaylarını analiz etmek için Hesaplamalı Akışkanlar Dinamiğinin (CFD) yaygın şekilde kullanılmasına olanak sağlamıştır. Ismael A. ve arkadaşlarının 2015 yılındaki deneysel çalışmasından elde edilen sonuçları karşılaştırmak ve doğrulamak amacıyla yakalı köprü ayağı için sayısal bir model oluşturulmuştur. Bulgular, yakalı köprü ayağı kullanılması halinde yerel oyulmanın azaldığını göstermektedir.

Anahtar Kelimeler: Oyulma, Flow 3D, Dairesel ayak, Burunlu ayak, Yaka

"Dedicated to my family"

ACKNOWLEDGEMENTS

I extend my heartfelt gratitude to Prof. Dr. Mustafa GÜNAL for his invaluable guidance, encouragement, and support throughout my thesis journey. His expertise and mentorship have been instrumental in shaping my research.

I would also like to express my deepest love and appreciation to my family for their unwavering support and constant encouragement. Their belief in me and their best wishes have been my driving force, and I am truly grateful for their presence in my life.

TABLE OF CONTENTS

Page

LIST OF TABLES

LIST OF FIGURES

LIST OF SYMBOLS

D_p	Pier diameter
h	Depth of water flow (m)
Q	Discharge (m^3/s)
L	Ratio of the pier length to the pier width
Fr	Freunde number
Re	Reynolds number
Re*	Shear Reynolds number
T	Time (min)
Gs	Specific Gravity of sand
ds	Local scour depth (m)
U	Velocity of water flow (m/s)
U_c	Critical velocity (m^2/s)
d_{50}	Median particle Size diameter of the sediments (mm)
a	Size of the Sediment
U_c^*	Critical Shear velocity (m/s)
σ_g	Standard deviation of the sand size
G_s	Gravity of the sediment particle (m/s^2)
ρ_s	Density of Sediment and correspondingly (kg/m^3)
ρ	Water density (kg/m^3)

LIST OF ABBREVIATIONS

CFD	Computational Fluid Dynamics
FAVOR	Fractional Area Volume Method
VOF	Volume of Fluid
FHWA	Federal Highways Administration
(CP)	Circular Pier
(CPC-2)	Circular Pier with Collar two Times the Pier Diameter
(CPC-3)	Circular Pier with Collars Three Times the Pier Diameter
NP	Nosed Pier Model
(NPC-2)	Nosed pier model with collar two times of the pier diameter
(NPC-3)	Nosed pier model with collar three times of the pier diameter

CHAPTER I

INTRODUCTION

1.1 Overview Background on the scour

The bed of rivers or streams around the world can change constantly so under these circumstances the engineers had to find a system to drain water efficiently without endangering the infrastructure. Even so, riverbed sediment which is naturally eroded by the flowing water, also transported and deposited river sediments, changing the height of the riverbed and its boundaries. Bridges are a vital element of the infrastructure of a country, it is crucial to protect these bridges from problems. Scour is one of the most problems against bridges. Scour is defined as a natural phenomenon that occurs in rivers because of the water flow. Water in motion can cause erosion, leading to scouring, which is the removal of particles from the bed and sides of the stream, including those near bridge piers and abutments. Scouring is a major cause of bridge failure and can lead to the formation of holes that undermine the foundations of bridge piers and abutments during significant flood events (Tulimilli., 2003). Affording to the United Nations Environment Program in 2000, soil erosion is a major

There have been several reported cases of bridge pier failure due to scour in the United States and worldwide. For the United States, scour has been identified as a contributing factor in the disaster of numerous bridges, including the Tacony-Palmyra Bridge in Pennsylvania, the Schoharie Creek Bridge in New York, and the Mississippi River Bridge in Minnesota as shown in Figure 1.1.

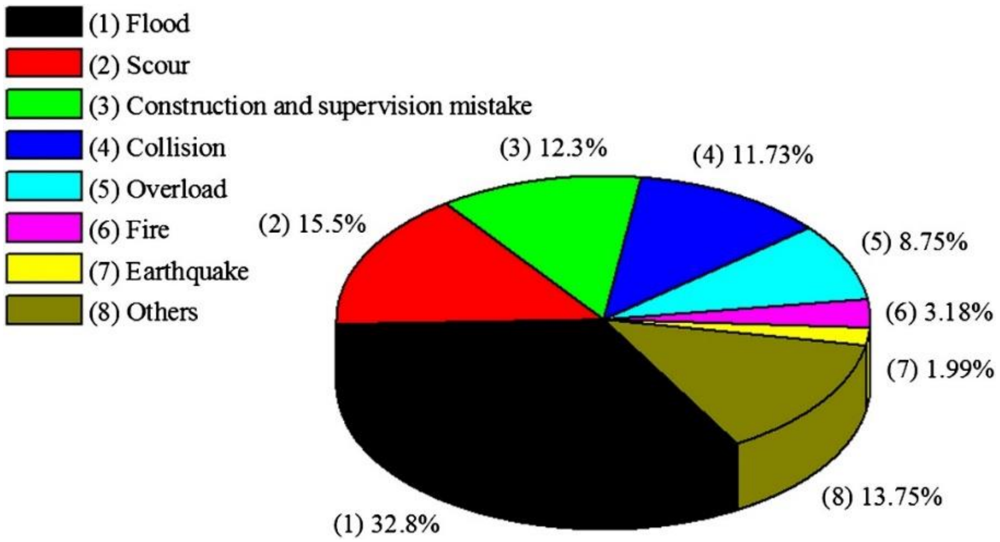

Figure 1.1 Reasons of the 503 reported bridge collapses in the United States from 1989 to 2000 (Wardhana, Hadipriono 2003).

According to Breusers' (1977) statistics, it was shown that scour accounts for 60% of the causes of bridge failures, making it the most frequent reason for bridge collapses. Scour depth refers to the reduction in sediment levels near bridge piers or other hydraulic structures.

1.2 Scour and its Classification

It is a general phenomenon occurs due to the flow of water where Sediment is being moved. Scour generally influences by the effects of abutments and piers when water passes across these structures and a net change in the bed elevation is observed. When the bed elevation decreases due to the erosion of bed then it is called as degradation where the increase of bed elevation due to the deposition of Sediment is called as aggradation.

1.3 Local Scour

Near a pier within a uniform open channel flow, the flow pattern undergoes a transition to a dynamic and intricate state as a scour hole takes shape around the pier, as noted by Bozkus (2004). The primary mechanisms contributing to scour around piers involve the downward flow at the upstream face of the pier and the formation of horseshoe vortices at the base of the scour hole, as highlighted by Muzzammil (2004). The downward flow transports sediment away from the pier's base, leading to the creation of a scour pit, and interacts with the incoming flow, resulting in the formation of a complex vortex configuration, a phenomenon documented by Whitehouse and Harris (2014). This vortex pattern extends around the downstream sides of the pier. The pivotal factor driving the scouring process is the downward flow reaching the bed, as elucidated by Melville and Raudkivi (1977). On the upstream side of the pier, the velocity of the approach flow diminishes to zero, establishing a stagnation point.

The decrease in flow speed from the surface to the bed leads to a reduction in stagnation pressure on the pier's face, creating a downward pressure gradient. This gradient drives a vertical jet-like flow down the face of the pier. The presence of the pier induces intense vortex movement near its base, entraining bed sediments. As the scour develops, the rise in local flow depth reduces the erosive motion at the bed, resulting in a decrease in the scour rate until a balance is reached (Lauchlan and Melville, 2001). The three types of statues mentioned directly above contribute to the thorough cleaning around the bridge piers.

Local scour can be of two types:

1. Clear-water Scour: This occurs when there is no sediment movement, and Sediment is not transported to the scour-prone zone.
2. Live-bed Scour: In this type, Sediment is transported with the flowing water, leading to a decrease in the scour's height. Achieving an equilibrium condition takes time for this type of scouring, and the depth of the scour oscillates around a mean position.

1.3 Scope of Thesis

The primary objective of this study is to conduct a numerical simulation based on the research conducted by Ismael.A.at al, 2015. Their research aimed to identify a cost-effective bridge pier shape that reduces local scour around the pier. In line with their work, this study selects two specific piers namely (circular pier and noise pier) for simulation and investigates adding collars for each pier to evaluate their impact on the reduction of scour depth.

Subsequently, two types of collars (Circular Collar and Airfoil-Shaped) will be added as attachments for each selected pier to estimate the possible effect on reducing scour depth around the bridge pier. The outcomes of this simulation will be compared with results from experimental investigations to establish the suitability of the Flow-3D software for comprehensively analyzing scour phenomena.

1.4 contribution of the study

This study is expected to provide contribution to reducing local scour around bridge pier by using collar research in the world. The proposed bridge pier with collar will give idea about reducing scour and give detailed information about scour mechanism.

The main objectives of this study are as follows:

- To conduct a numerical simulation based on the research by Ismael and Gunal in 2015, with the aim of identifying a cost-effective bridge pier design that reduces local scour around the pier.
- To select two specific types of piers (circular and nosed) for simulation and assess the potential impact of adding collars to each pier on the reduction of scour depth.
- To examine two types of collars (Circular Collar and Airfoil-Shaped) as attachments for each selected pier to estimate their effect on reducing scour depth around the bridge pier.
- To compare the simulation outcomes with results from experimental investigations to determine the suitability of the Flow-3D software for a comprehensive analysis of scour phenomena.
- The results from the new models will be compared to reference the model (circular pier model)

1.5 Thesis Outline

This thesis is organized into five chapters. The content of the chapter is summarized below:

Chapter 1: Overview

In this opening chapter, the study's objectives and thesis framework are outlined.

Chapter 2: Literature Review

The second chapter covers previous researches related to scouring, encompassing different types of scours, sediment movement around pile foundations, the impact of bridge pier design and geometry on scour reduction.

Chapter 3: Methodology and Experimental Procedures

This section provides a detailed account of the methods and procedures employed in both experimental and CFD modeling. It includes meshes' setup, boundary conditions' definition, and relevant physical parameters.

Chapter 4: Results

Within this chapter, a thorough examination and discourse of the results pertaining to the application of the collar method for diminishing local scour depth around the bridge will be provided.

Chapter 5: Conclusions and Recommendations

The concluding chapter encapsulates the principal findings extracted from both investigations and presents insightful suggestions for potential avenues of future research exploration.

CHAPTER II

LITERATURE REVIEW

2.1 Introduction

Scouring causes, the movement of the sediment bed from the upstream of the flow direction and the movement weakens the pillar structure and making the structure risky. Extensive investigation into this phenomenon has been conducted over the preceding few decades and being continued. The scour background, failure statistics, and terminology of scour and its classification was reviewed within the initial chapter, and subsequently in the second chapter, there will be an exploration of specially discuss the scour mechanism, factors affecting bridge scour countermeasures methods and basic theories related to the transportation of the Sediment and the previous studies related to scouring.

The phenomenon of scouring around bridges has emerged as a significant factor contributing to instances of bridge structural failure, as delineated in Figure 2.2. Over the course of the previous three decades, the United States has witnessed a substantial number of bridge collapses, exceeding 1,000 in total. A notable proportion, approximately 60%, of these instances has been attributed to scouring effects in proximity to bridge piers, a finding highlighted in the investigation conducted by Shirhole and Holt in 1991. This concern was exacerbated by a comprehensive inquiry undertaken by the Transportation Research Board in 1997, revealing a substantial total of 488,750 bridges spanning over streams and rivers across the United States. The economic implications of such failures related to scouring were estimated to reach an annual cost of $30 Million, according to estimates presented by Lagasse and colleagues in 2001.

Figure 2.2. Collapse of the Schoharie Creek Bridge due to flood in 1987 (USGS 2012).

The phenomenon of scouring around bridges has emerged as a significant factor contributing to instances of bridge structural failure, as delineated in Figure 2.2. Over the course of the previous three decades, the United States has witnessed a substantial number of bridge collapses, exceeding 1,000 in total. A notable proportion, approximately 60%, of these instances has been attributed to scouring effects in proximity to bridge piers, a finding highlighted in the investigation conducted by Shirhole and Holt in 1991. This concern was exacerbated by a comprehensive inquiry undertaken by the Transportation Research Board in 1997, revealing a substantial total of 488,750 bridges spanning over streams and rivers across the United States. The economic implications of such failures related to scouring were estimated to reach an annual cost of $30 Million, according to estimates presented by Lagasse and colleagues in 2001.

In the case of the United States, Alabi's 2006 study stated that flood damage restoration on highways costs an average of $50 million each year. Additionally, floods have also contributed to bridge failures in Turkey during the last few decades, with incidents occurring in Trabzon, Malatya, Bartın, Hatay, and Mersin between 1990 and 2001 Kirwan, G., et al. (2010).

In 1914, Gilbert presented the foundational equation for estimating sediment transport. Subsequently, a range of equations have been introduced to model sediment transportation within open channels. These equations have been devised to accommodate various sediment grain sizes under conditions of steady state and uniform flow. Particularly, equations for total sediment load have gained prominence among engineers due to their applicability across diverse sediment transport scenarios, without differentiation between bed load and suspended load. It's worth noting that some equations are specifically tailored for either suspended load or bed load, as discussed by Graf (1984).

There has been significant research done by Melville and Chiew (1999), Kothiary et al (1992a, 1992b), Laursen (1962, 1963),, Vittal et al (1994), (Chang 1988), Garde and Raju (1985), Ram (1999), Johnson and Bilal (1996), Dey et al (1995), Sheppard and Jones (1998), Dey, S. (2007)., Parola (1996), and Lim and Chiew (1999) and authors have studied various aspects of scouring on aspects of local scour, including time-based and equilibrium scour, clear water and live bed scour, scour in uniform and non-uniform bed materials, and scale effects in pier scour. Many empirical equations and mathematical models have been developed to predict scour depth around piers, with the goal of estimating the ultimate scour depth. In recent years, studies have been made to lessen scour via piers of various shapes, geometries, and orientations.

2.2 Local Scour Mechanism

The maximum failures of bridges occur for the scouring which removes the Sediment from the base of piers. And research are being carried out across the world to make the pier design safe and economical. When water is flowing two bridge the pier there creates a stagnation point at the intersection between the pier and the direction of the flow where velocity comes to complete rest Cook, W. (2014).

The velocity distribution of the approaching flow varies from zero at the bed surface up to the maximum at the surface of water that creates a pressure gradient from the bottom to the top. This change in pressure creates vortex at the bottom of the pillar that sweeps Sediment from the region and the vortex looks like a horseshoe. For that reason, this type of vortex is called horseshoe vortex Shahriyar, M. A. (2021). The basic mechanism leading to local scouring on piers or abutments is the creation of vortexes. Water deposition on the upstream face and subsequent flow acceleration around the nose of the pier or abutment contributes to vortex formation. When the transport rate of Sediment away from the local area is higher than the transport rate into the region, a scour hole forms. As the scouring depth increases, the frequency of the vortexes decreases and hence the transport rate decreases. Scouring ceases as equilibrium is restored and the scouring void will not grow further. A traditional vortex around a pier is: (Horseshoe vortex, Wake, Bow wave, Trailing vortex)

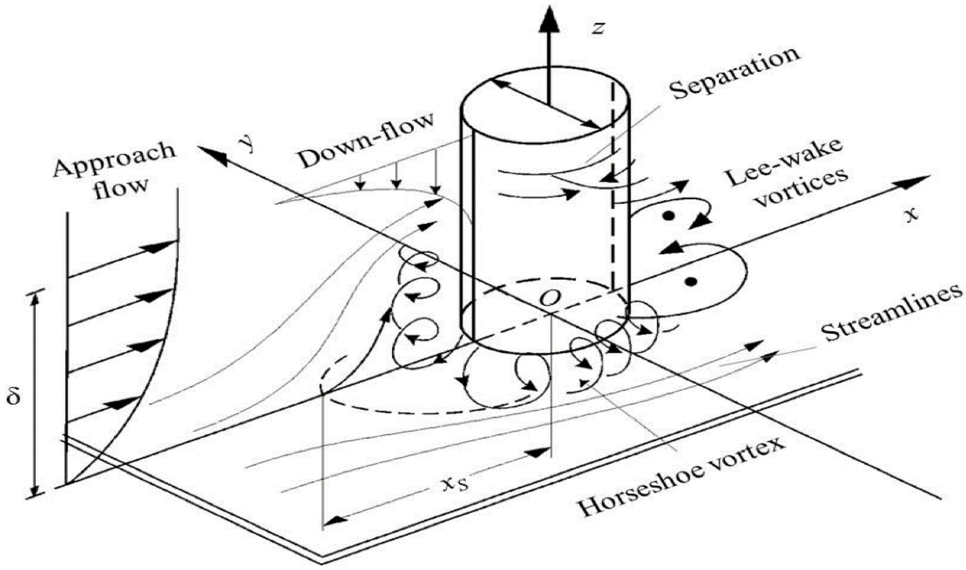

Figure 2.1 Mechanism of local scouring Cook, W. (2014).

As the scour hole around a pier in a uniform open channel flow increase, the flow beginning nearby the pier becomes more complex, as observed in the study by Bozkus and Osman (2004). The primary essentials that contribute to the occurrence of pier scour encompass the downward flow experienced at the upstream face of the pier and the subsequent development of horseshoe-shaped vortices at the base of the scour hole, as documented in the research conducted by Muzzammil et al. (2004).

The downflow causes a scour hole by displacing Sediment from the base of the pier when it reaches the channel bed. A highly intricate vortex system develops when the downflow interacts with the incoming flow as it approaches the channel bed, as explained by Hirshfield (2015). Subsequently, this system of vortices continues its downstream extension along the lateral aspects of the pier. The downflow reaches its maximum strength just below the natural bed level, and its effect on the bed is the primary mechanism for scouring, as highlighted by Melville and Raudkivi (1977).

At the stagnation point located upstream of the pier, the incoming flow velocity diminishes to zero, leading to an elevation in pressure on the pier's frontal surface. The stagnation-induced pressure on the pier's leading face diminishes progressively as the velocity experiences a decrease from the surface to the bed, primarily due to the downward-directed pressure gradient. This pressure gradient initiates a downward motion of the flow along the pier's surface, resembling the behavior of a vertical jet.

Moreover, the presence of the pier induces strong vortex motion, leading to the entrainment of bed sediments near the pier base, as observed by Lauchlan and Melville (2001). Figure 2.1 provides a visual representation of the flow dynamics and scour pattern occurring around a circular pier, influenced by the presence of currents.

2.3 Flow Field Motion Around Bridge Piers

When encountering an obstruction, the flow field undergoes a division into three distinct motion patterns: down-flow, the formation of a horseshoe vortex, and the development of wake vortices. These patterns are elaborated upon in the subsequent sections.

2.3.1 Down Flow in the Front of the Piers

Upon come across the bridge dock frontage, the flow field causes an elevation in the water flow depth, leading to the creation of a stagnation point at the front surface of the bridge pier. Consequently, a pressure variation initiates between the upstream and stagnant sides of the pier (Yanmaz, 2002). Furthermore, the depth of flow is contingent on the fluid's profile and velocity. As the flow velocity diminishes in front of the pier, the associated pressure also decreases, influenced by the approach velocity.

2.3.2 Horseshoe Vortex

The term "horseshoe vortex" is utilized in the literature to depict the flow pattern around a pier due to the shape of the eddy (Zhao et al., 2010). The development of the horseshoe eddy system occurs naturally following the creation of a scour hole (Ozalp, 2013). As downstream flow interacts with the incoming flow, the horseshoe vortex system takes shape. This vortex flow proceeds downstream along the edges of the pier, as illustrated in Figure 2.4. The strength of the horseshoe vortex is influenced by factors such as pier shape, geometry, and turbulent flow (Yanmaz, 2002). In essence, a pier with a blunt nose generates a significant pressure gradient, initiating the mechanism described above. This vortex forms when the bridge pier aligns with the flow path and the upstream side of the pier is characterized by a sharp nose, with the eddy's characteristics varying depending on the pier's attributes (Breusers, 1977).

2.3.3 Wake Vortices

The wake vortexes formed when the flow split takes place when the flow passes on the edges of a pier, as clarify Figure 2.4. These wake vortexes are also responsible for material erosion around the bridge pier. Wake vortexes migrate downstream and lead to the transportation of sediments by downstream and horseshoe vortex (Melville and Coleman, 2000).

Such vortices are responsible for generating holes near the piers. This form of erosion damages many of the bridges (Hamidi and Siadatmousavi, 2017). As shown in Figure 2.1 Mechanism of local scouring and Figure 2.2 shown forms of vortexes around piers.

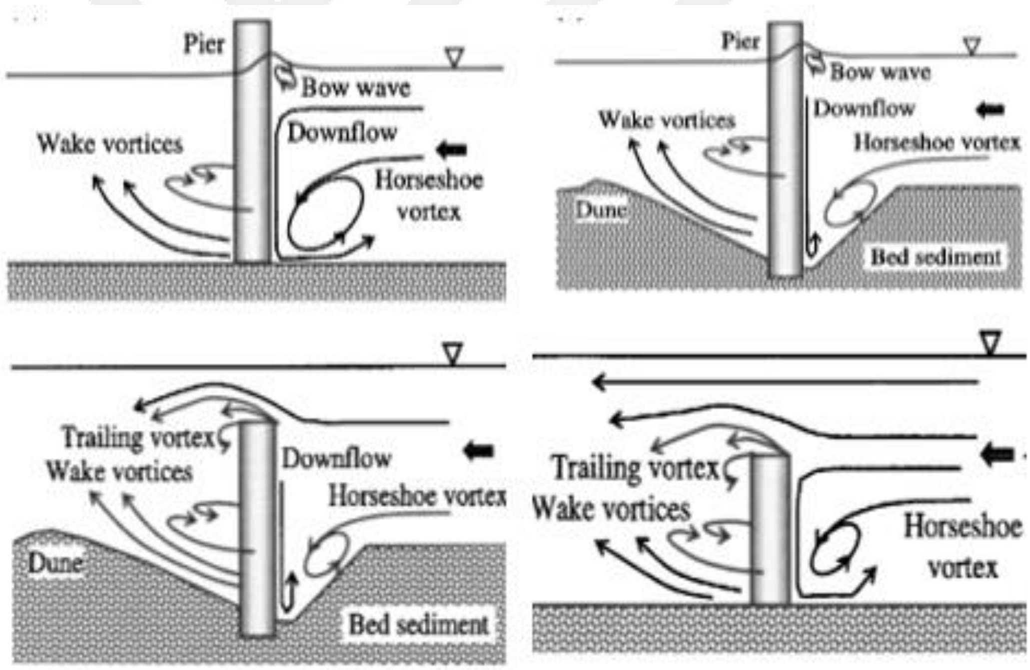

Figure 2.2 Flow movement and scour formation are observed around a circular pier, as documented by Melville and Coleman (2000).

2.4 Parameters Effect on Scour Depth

Several studies product by (Barbhuiya, 2004) (Richardson and Davies 1995) and Lagasse et al. (2001) have shown the local depth around the bridge piers is influenced by several parameters like;

2.4.1 Flow Velocity

The velocity is regarded as one of the most essential parameters that affect the depth of the scour, also both the shear velocity (U) and the number of Froude (Fr). Brownlie, W. R. (1983). decided that the number of Froude is enough to reflect the velocity influence of maximum velocity. Through this concept, the depth scoring in the natural channel, considering Froude number in their investigations and also, regarding shear velocity, reflect the current's ability to scouring it appears after earlier studies and literature similar (Rajaratnam, N., & Nwachukwu, B. A. (1983), (Mccrquodale,1975), Froehlich, D. C. (1989), in the situation of consuming clear water the maximum depth of scouring takes place when ($U=U^*_c$) this indicates that the flow velocity equals the critical velocity, and this profundity is referred to as threshold peak Peck, R. B. (1996 Singh) and Maiti. (2012).

In experimental efforts to establish the link among scoring profundity as well as Froude number, the scour round the spherical dock was determined that depends on. (a) channel bed soil characteristics, (b) pier design and size, (c) Froude number of flows, (d) scouring is also affected by the vortex creation round the piers and its type.

2.4.2 Flow Depth

Flow profundity is regarded as one of the criteria of efficiency for the depth of scouring (Laursen., 1952). Some research indicate that the ratio of the shear velocity over critical velocity ($\frac{U^*}{UC}$) is constant. The scouring depth reduces with a depth drop and explains that scouring depth is immediately proportional to the flow depth in the sediment-water (Tey, 1984), (Wong, 1982), and (Kandasamy, 1989).

2.4.3 Reflectivity Gradation and Size of Sediments

The size of the Sediment will be matched to the diameter of the pier in a theoretical examination. This is to ensure that the size of the Sediment does not affect the diameter of the bridge piers, if this result of the equation is more than 50 then there is no influence between the size of Sediment and depth of scouring (Ettema, 1980).

$$\frac{D}{a.(d50)} > 50 \qquad (2.2)$$

D= diameter of Pier, and a= size of the Sediment. Table 2.1 clarify the size classification of the sediment particles.

Moreover, the depth of scour tends to increase when the diameter of the sediment particles exceeds 2 mm, as indicated by Wong (1982). Ramu (1964) studied the effect of particle gradation and found that equilibrium scour depths varied with different standard deviations of grain size for a consistent canal bed grain size. Ahmed (1998) also noted that the standard deviation of the riverbed sediment had a significant influence on the equilibrium scour depth. The following equation provides an explanation for the depth of scour under clear water conditions:

$$\mathrm{Ds.}(\mathrm{g}/\mathrm{D}) = \mathrm{K}\,\sigma\,\mathrm{Ds}/\mathrm{D} \qquad (2.3)$$

Where:

Ds: represents the equilibrium scour depth, g: is the standard deviation of the sediment particle sizes., K= is a coefficient that depends on (σg), D= is the diameter of the pier.

Table 2.1 Classification of the Sediment Particles.

Practical Name	**Range Size**	**Loose Sediment**	**Consolidated rock**
Boulder	> 256 mm	Gravel	Conglomerate or breccia (depends on rounding)
cobble	64-256 mm	Gravel	
pebble	2-64 mm	Gravel	
sand	1/16-2 mm	sand	sandstone
silt	1/256 - 1/16 mm	silt	siltstone
clay	$< \frac{1}{256}$ mm	clay	Claystone, mudstone, and shale

2.4.4 Bridge Pier and Attack Flow Angle

delves into the interplay between the bridge pier configuration and the angle of attack of the flowing water Tison, L. J. (1961) Conducted an extensive study on scour around bridge piers, suggesting that the curvature of streamlines plays a crucial role in influencing the scour phenomenon. Shen et al. (1969) classified pier shapes into two types:

1. Blunt-nose piers exhibit a strong horseshoe vortex system, leading to localized scour depths near the upstream pier surface. The geometry of the piers at the

upstream side significantly affects the depth of scouring. Additionally, the length of the pier has minimal impact when the pier is positioned close to the flow with a blunt-nose shape.

2. Influence of pier shape and attack flow angle on scour depth, the shape of a bridge pier and the angle at which the flow approaches it play crucial roles in the scour depth development. Sharp-nose piers, characterized by their streamlined profiles, exhibit a relatively weaker horseshoe vortex structure, resulting in the localization of maximum scour depth closer to the downstream face of the pier. Laursen and Touch (1956) emphasized that in the case of elongated piers facing a pronounced attack angle of the flow, the position of the maximum scour depth shifts along the downstream direction, eventually settling near the edge of the pier. This observation highlights the intricate interplay between pier geometry and the incident flow angle in determining scour patterns and depths.

A previous study by Chabert and Engeldlnger (1956) investigated scouring around six different pier types (shown in Figure 2.3 and Figure 2.4). The results of this study revealed three main points:

1. Pier shapes in Group 1 (including pier shapes 1, 2, 4, and 6 shown in Figure 2.5) exhibited similar maximum scour depths under comparable flow conditions.
2. For pier shape 3, the maximum scour depths ranged from 33% to 86% of those observed for the matching flow velocities in Group 1. Higher flow velocities resulted in lower scour depths.
3. Influence of pier shape on scour depth variation in the context of pier shape, the fifth configuration exhibited noteworthy disparities in maximum scour depths, ranging from 50% to 100% compared to those observed in Group 1 for equivalent flow velocities. Notably, as flow velocities escalated, the scour depths also exhibited a corresponding increase.

Figure 2.3 shows the shapes of the piers and the influence of the attack angle on scouring.

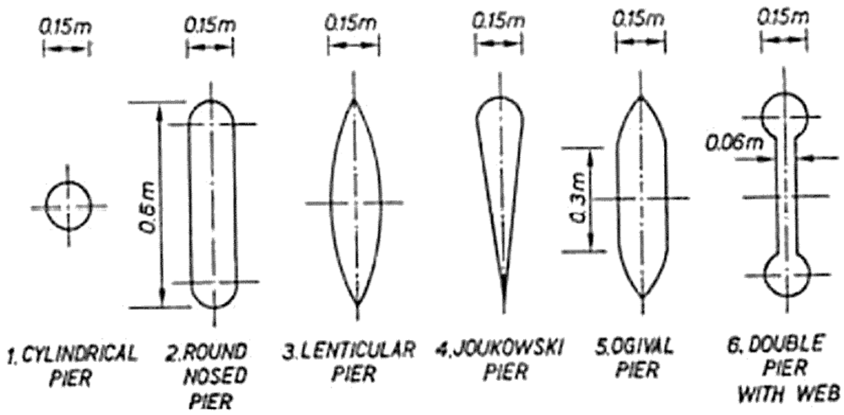

Figure 2.3 Several piers' shapes were examined for scour reduction (Chabert and Engeldlnger, 1956).

As depicted in Figure 2.4, alterations in scour depth exhibit a trend of reduction through the streamlining of piers characterized by a zero-attack angle; nevertheless, this advantageous trend becomes less prominent for attack angles exceeding 10°. A notable exception arises in scenarios involving the arrangement of two circular piers spaced at a distance equivalent to three times the pier diameter, where the influence of the angle of attack on scouring remains limited. A pioneering investigation undertaken by Paintal and Gard in 1956 revealed intriguing insights into this phenomenon. Their study indicated that the rear aspect of the pier has negligible impact on scouring, in contrast to the pivotal role played by the pier's upstream nose.

Their experimental analysis encompassed piers exhibiting an upstream triangular configuration with apex angles spanning from 15° to 180°. Their results indicated a direct relationship between increased apex angles and augmented maximum scour depth. Furthermore, the length of the pier exhibited no discernible influence on the rate of maximum scouring depths, given the specific pier shape and dimensions investigated, which incorporated sediment particles of 2.5 mm in diameter.

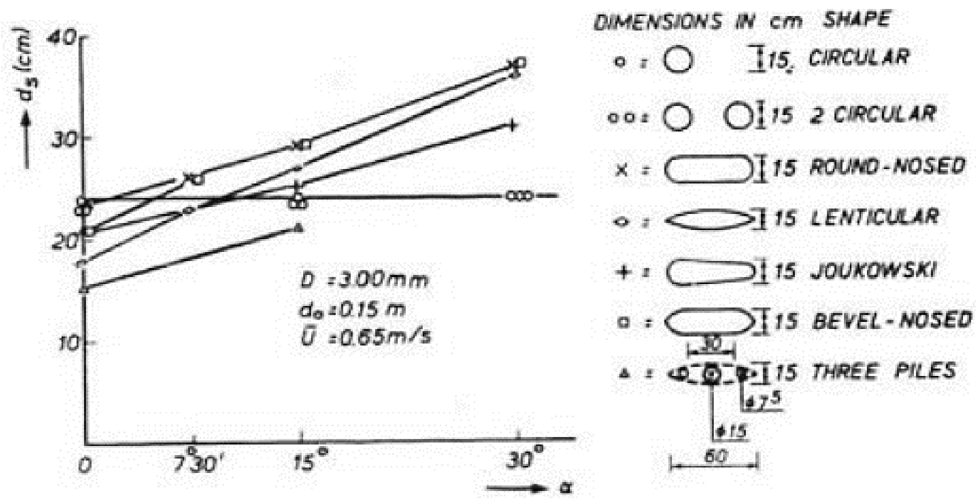

Figure 2.4 Effect of the angle of attack with the depth of scouring for different pier shapes (Chabert and Engeldlnger, 1956).

2.4.5 Variation Time and Scour

The concept of equilibrium scours refers to a state where the depth of scouring remains relatively constant over time. This idea is frequently discussed in the literature and has been explored by various researchers. For instance, Franzetti et al. (1982) addressed the state of equilibrium as the condition where no significant further adjustments in scour depth occur as time progresses. The occurrence of equilibrium is often associated with the absence of significant changes in scouring dynamics.

Local scour can be categorized into two main sediment transport scenarios: clear water and live bed. As depicted in Figure 2.7, in live-bed conditions, equilibrium scour depth is established when the average outflow of sediment particles from the scour hole matches the average inflow. This equilibrium state is reached relatively swiftly in comparison to scenarios involving clear-water flow. In live-bed conditions, the equilibrium scour depth experiences fluctuations around an overall mean value. On the other hand, in situations with clear-water flow, equilibrium scour depth is reached when the flow becomes insufficient to dislodge sediment particles from the scour hole.

Chabert and Engeldinger (1956) concluded that equilibrium is achieved when the scour depth remains relatively stable without significant fluctuations over time. Ettema introduced a categorization of three distinct phases characterizing the scour mechanism, providing a comprehensive understanding of its dynamics.

1. The initial stage is defined by quick scouring caused by downflow at the pier's upstream face; the horseshoe vortex plays little influence, and sediment transport begins at the pier's sides.

2. The major stage is controlled via the horseshoe vortex activity; throughout this phase, scour happens in a narrow section round the pier. Also, the hole of scour grows, the strength of the horseshoe vortex and the downflow gradually develop powerless to transfer Sediment beginning from the bed erosion area.

3. The equilibrium stage is gotten when no additional important progress in the scour hole occurs.

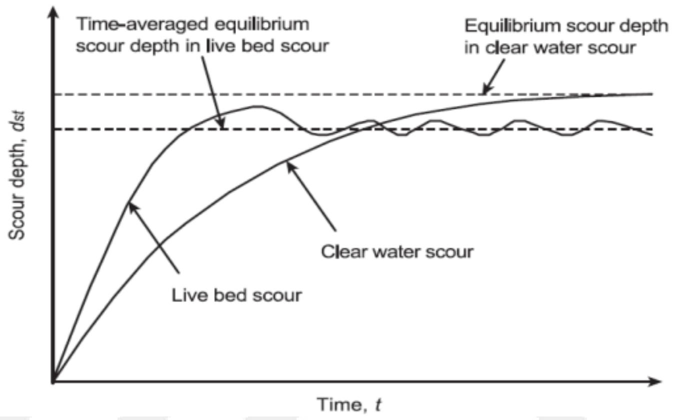

Figure 2.5 Time and Scour depth progress of live-bed and clear-water scour (Chabert and Engeldinger 1956).

They discovered that, even after the absence of the equilibrium circumstances, the constant deepening of a balancing hole takes happen rather slowly. With clear-water scour conditions and average of the shear stress with the weight of water and turbulence stresses generates balance simultaneously. Melville and Coleman (2000) In laboratory tests using clearwater condition, indicate the essential parameters to attain equilibrium scour condition, requiring the test to continue for many days without interruption. Bozkus and Osman (2004) Evaluate the time limit of the studies conducted should be limited to 2 hours based on the experiments performed; despite the fact that takes more than 2 hours 0.to reach the final equilibrium depth, they discover that the rate of the scour depth hole has decreased after 2 hours. Mia and Nago (2003) stated that if the scour progression in one hour is less than one millimeter, the experiments can be stopped. Because the trend of scour hole development is asymptotic, some researchers have decided where to stop the experiments. The proposal has been formally recognized by Melville and Chiew (1999).:

$$\frac{\mathrm{d}(dse)}{\mathrm{d}t} \leq \frac{0.05D}{24hr} \tag{2.4}$$

From the previous equation, it can simply be stated that when the change of scour hole does not go above 5% of the pier diameter in 24 hours, the experiment test is assumed to reach equilibrium.

2.5 Review of Countermeasures Method of local Scour

Local scour is soil erosion around the base of a bridge due to the flow of water. This can be a severe issue, as it can destabilize the structure and cause it to collapse. Several methods can be used to counter the effects of local scour, including the following:

- Riprap revetment involves placing large stones or other materials around the structure's base to protect against erosion. The stones absorb the flowing water's energy and prevent soil erosion.
- Grout bags: These are bags filled with grout placed around the structure's base. The grout hardens over time, forming a protective barrier against erosion.
- Scour countermeasures: These are specialized structures or devices designed to prevent erosion around the base of a bridge or other structure. Examples include scour aprons, concrete or stone slabs placed around the base of the structure, and scour curtains, which are flexible barriers placed in the water to protect against erosion.
- Sediment traps are structures designed to trap Sediment in the water before it reaches the base of the structure. This can help reduce the amount of erosion that occurs around the structure's base.
- Restoration of streambanks: In some cases, erosion may be caused by the destabilization of the streambank itself. In these cases, it may be necessary to restore the streambank to prevent erosion from occurring. This can be done through the use of vegetation, rock revetments, or other measures.

The researchers have identified two principal countermeasure categories used to decrease the scour around bridge piers: Altering of Flow and the Bed armoring

(Tafarojnoruz 2010). Flow-altering measures are designed to reduce the intensity of the downflow and the vortex of the horseshoe (Ferraro, D., Tafarojnoruz, A., 2013). Employing altering flow devices reduces the depth of the scour depth, and the shear stresses on the bad of the river and the scour area of the pier are decreased due to the altering flow pattern surrounding it (Mubeen., 2013). also, Tafarojnoruz, Gaudio, and Dey (2010) classified the flow-altering methods into four categories, the previous studies conducted on the many methods, in this thesis focuses of one methods of countermeasures which is collar pier attachment, it will be explained by reviewing the literature studies:

2.6 Collars Attachments to Pier

The streamed resistance can be considerably improved using bed armor counter measurement attachments. The equipment or attachment of the pier includes collars or horizontal platforms, threading and fittings (Tafarojnoruz 2010). collars cases used in this study will be explained by reviewing the literature studies. As shown in Figure 2.9 Shape Pier with collar, the collars were contacting with the piers and utilized to divert flowing of water away from them (Melville 1999). Many investigations research was carried out to establish the ideal diameters and location for placement, the collar directly affects the downflow by reducing the depth of scouring and scour rate (Mubeen., 2013). The collars cover the entire pier, also the plate is commonly just contacting to the face of the pier. collar located just at otherwise just below the natural bed level to reverse and prevent the scouring from continuing after depth the collar and pier (Tafarojnoruz 2010).

Increasing the diameter of a collar and positioning it below the sediment bed level yielded a significant improvement in reducing scour depth. Additionally, the particle size of the sediment played a role in influencing the collar's effectiveness, as noted by Gris (2010). The efficacy of scour reduction by the collar is influenced by its diameter, although practical considerations guide its size selection. Plates affixed to the pier's face serve to mitigate the downward flow, thereby initiating the formation of a horseshoe vortex. Kumar's research (1999) underscores that a larger scour hole is formed at the upstream face of the pier when utilizing a smaller collar diameter positioned higher up, as opposed to adopting a larger collar diameter at a lower height (Kumar, 1999).

A laboratory-based experimentation involving both rectangular and circular collars corroborated these findings. The outcomes revealed a 79% reduction in scour depth for both circular and rectangular collars. Notably, positioning the collar beneath the river bed surface yielded the most pronounced reduction in scour depth (Akib, S., Jahangirzadeh, A., & Basser, H., 2014).

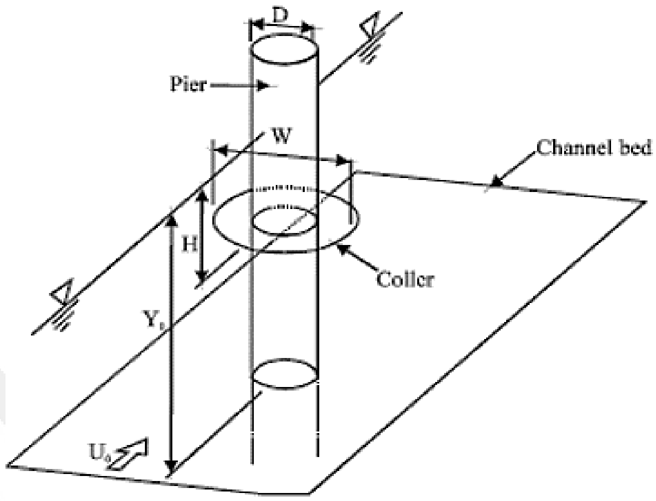

Figure 2.6 Shape and Positioned the collar around circular pier (Mashair, 2004).

2.7 Sediment Properties

Here two conditions exist like live bed scour and clear water scour. And it can't be predicted by observation. In case of live bed scour Sediment are transported with water where in clear bed scour Sediment are not transported with water. Other than these, particle size, distribution for non-cohesive sediments, spatial distribution of sediment size are important factors.

2.8 Scour Prediction Governing Equations

There are several equations that are commonly used to predict the depth and extent of scour around bridge piers and other structures. These equations take into account factors such as the flow velocity, depth, and type of soil at the site, as well as the size and shape of the structure. Some of the most commonly used equations for scour prediction include:

- The Prandtl-Meyer equation: This equation predicts the flow velocity and depth of scour around a pier based on the flow characteristics and the size and shape of the pier.

- The Chezy equation: This equation estimates the flow velocity in a channel based on the roughness of the channel and the slope of the channel bed.
- The Strickler equation: This equation estimates the scour depth around a pier based on the flow velocity, the size and shape of the pier, and the characteristics of the soil at the site.
- The Shields equation: This equation estimates the critical flow velocity at which Sediment begins to be transported by the flow. This can be used to predict the onset of scour around a pier.
- The Van der Meer equation: This equation estimates the scour depth around a pier based on the flow velocity, the size and shape of the pier, and the characteristics of the soil at the site.
- It is important to note that these equations are only estimates, and that actual scour depth and extent can vary significantly from the predictions made by these equations. In practice, engineers often use a combination of these equations and other methods, such as physical modeling and field observations, to predict scour and design countermeasures.

Numerous empirical equations have been formulated to estimate the local scour depth around bridge piers, as outlined by McIntosh (1989). These equations are categorized based on the type of local scour, distinguishing between clear-water scour and live-bed scour. The development of local scour equations involves various approaches, including curveting and regression methods, to calculate the maximum scour depths. Notably, there exist several equations aimed at estimating the scour depth, which are as follows:

1- Breusers equation

The local scour depth equation developed by Breusers, H. N. C. (1965). Breusers concluded, that the maximum scour depth affected by pier diameter where the maximum scour depth was about 1.4 times the pier diameter.

$$d_s = 1.4b \tag{2.1}$$

where b is pier diameter and d_s maximum scour depth.

2- Laursen equation

Laursen and Toch (1956) rest on on investigational study for the development scour equations through the consideration of the flow depth in computing scour depth, but Shen (1966), while Shen (1966) depend on the velocity for development scour equation by including Froude number. The folloing formula (Laursen and Toch) are for square-nosed piers Hamill, L. (1998).

For Live bed-scour:

$$d_{sp} = 1.5\ b_p\ 0.7Y0.3 \tag{2.2}$$

For Clear-water scour:

$$d_{sp} = 1.35\ b_p\ 0.7Y0.3 \tag{2.3}$$

Where, d_{sp} is the dock scour profundity (m), b_p is width of the pier (m), y is the depth of method flow (m).

While Shen II equation is written

$$d_{sp} = 3.4\ bp\ 0.67\ F0.67\ Y0.33 \tag{2.4}$$

where F is the Froude number of the approach flow.

3- Larras equation

Larras (1963) depends on field data several French rivers to developed Larras equation:

$$y_s = 1.42\ K_{S2}b0.75 \tag{2.5}$$

where K_{S2} is a coefficient based on the form of the dock nose (1.0 for cylinder-shaped piers and 1.4 for quadrangular piers) Where y_s and b in ft.

Larras measured scour profundity afterward a flood had accepted, there for the equation depends on pier thickness and shape individual (Shen and others, 1969).

4- HEC-18 equations

(Richardson and others, 1993) presents (HEC-18) equations based on experimental data for circular piers scour for development the scour.

$$\frac{ys}{yo} = 2\ K_1K_2K_3\left(\frac{b}{yo}\right)^{0.65} F_O\ ^{0.43} \tag{2.6}$$

where K_1 is a coefficient based on the shape of the pier nose (K_1=1.1 for square- nosed piers, 1.0 for circular nosed piers, and 0.9 for sharp nosed piers);

The coefficient for pier alignment is based on the ratio of pier length to pier width (L/b) and the alignment of the approach flow to the bridge pier (Richardson et al., 1993).

Table 2.2 Coefficient for pier alignment (K_2) (Richardson et al, 1993).

Angle	L / B = 4	L / B = 8	L / B = 12
0º	1	1	1
15º	1.5	2	2.5
30º	2	2.75	3.5
45º	2.3	3.3	4.3
90º	2.5	3.9	5

Table 2.3 Bed-condition correction factor (K_3) (Richardson et al, 1993).

Bed condition	Dune height	* K3
Clear-water scour	N/A	1.1
Plane bed and antidune flow	N/A	1.1
Small dunes	0.6 to 3.0 m	1.1
Medium dunes	3.0 to 9.0 m	1.1 to 1.2
Large dunes	> 9.1 m	1.3

*K_3 is a coefficient based on channel bed conditions.

5- Melville and Sutherland (1988)

Melville and Sutherland depend on investigational data for the development of equation, this equation called Melville and Sutherland equation

$$d_S = K_1 K_d \, K y \, K_a K_s \, b \tag{2.7}$$

In this equation, K1 is a coefficient that represents the intensity of the flow, Kd is a coefficient that represents the size of the Sediment, Ky is a coefficient that represents the depth of the flow, Ka is a coefficient that represents the alignment of the flow, and Ks is a coefficient that represents the shape of the pier. These coefficients are used in an equation to predict the scour depth around a pier.

Many empirical equations created to determining the local scour depth at bridge pier according to McIntosh (1989). Local scour equations are classified based on type of local scour if its clear water scour or live-bed scour, local scour equations can be developed using different methods like curveting and regression method to compute maximum scour depths. There are some equations to compute the scour depth wich Summered by table 2.4:

Table 2.4. Summary of predicted equilibrium scour depth equations

Researcher	Equations	Description
Breusers (1965)	$d_s = 1.4b$	ds are max scour depth b is pier diameter
Laursen and Toch (1956)	$d_{sp} = 1.5\ b_p\ 0.7Y0.3$	d sp is the dock scour depth (m), bp is width of the pier (m), Y is the profundity of approach flow, for live bed scour
Laursen and Toch (1956)	$d_{sp} = 1.35\ b_p\ 0.7Y0.3$	For clear-water scour
Shen II	$d_{sp} = 3.4\ b_p\ 0.67\ F0.67\ Y0.33$	F is the Froude number of the approach flow
Larras (1963)	$y_s = 1.42\ K_{S2} b^{0.75}$	K_{S2} is a coefficient constructed on the shape of the dock nose.
HEC-18 equation	$y_s / y_0 = 2\ K_1\ K_2\ K_3 \left(\frac{b}{y_0}\right)^{0.65} F0^{0.43}$	F is a Froude number K_1 K_2 K_3 is coefficient
Melville and Sutherland (1988)	$d_S = K_1 K_d\ K_y\ K_a K_s b$	
Raudkivi and Ettema(1983)	$y = 2.3bK\sigma$	where $K = f(\sigma_g) = 1$ for uniform sediment, σg= symmetrical standard deviation of the grain size distribution
Shen et al. (1969)	$y_{se} = 0.000223R_b^{0.619}$	where R_b = pier Reynolds number

2.9 Turbulence Modelling

It is a way of construction and use of a mathematical model for the estimate of effect of Turbulence in fluid flows. Turbulence consists of high frequency fluctuations and formation of different varieties of eddies with energy variation. It's a very complex process in fluid that depends on various causes like dynamic structure, flow area, approach flow velocity and others Turbulence is mainly characterized by Reynolds number. The high value of Reynolds number makes the flow turbulent in nature and in most of the situation are encountered with turbulent flow.

Various turbulence modeling approaches are available, and in this analysis, the Renormalized Group (RNG) turbulence modeling method has been employed. This method is recognized as a straightforward and efficient technique for establishing scaling of specific models and calculating corresponding critical exponents.

The RNG k-model, as introduced by Yakhot and Orszag (1986) and further developed by Yakhot and Smith (1992), presents an enhanced version of the two-equation k-model. It is particularly recommended for addressing a wide range of industrial scenarios. This model offers improvements in capturing transitionally turbulent flows, curvilinear flows, wall heat transfer, and mass transfer within the context of the Navier-Stokes equation for energy dissipation rate and kinetic energy. It extends the capabilities of the standard k-model.

The Renormalization Group (RNG) methodology is harnessed to formulate a nonlinear algebraic Reynolds stress model for Turbulence. This involves representing Reynolds stresses as quadratic functions of mean velocity gradients. The underlying objective of the renormalization group analysis is to develop a comprehensive theory of large-scale Turbulence that incorporates the impact of small-scale fluctuations by utilizing an effective or renormalized coupling constant and viscosity. This approach offers a more intricate comprehension of the intricate behaviors exhibited by turbulent flows.

The Yakhot-Orszag renormalization group has been specifically tailored for addressing non-linear turbulence equations, achieved through the evaluation of second-order Reynolds stresses within the Ɛ expansion of the Yakhot-Orszag theory. Its capacity to converge across different turbulent models renders it suitable for investigating the scouring process, which serves as a focal point in this research.

CHAPTER 3

METHODOLOGY

3.1 Introduction

The methodology used to simulate and analyze the scouring process around the bridge pier with two shapes is the main topic of this section, with two collar diameters. The analysis will be performed based on experiments by Ismael A. et al. (2015) at Gaziantep University's hydraulics lab to determine the depth and the scour around the bridge pier. The study uses a 3D numerical model of sediment scours using the Flow-3D program.

3.2 The Data Collection

Figure 3.1 shows flume in the experimental setup done by (Ismael A. et al (2015). The experiments were carried out in the following dimensions of a rectangular flume.

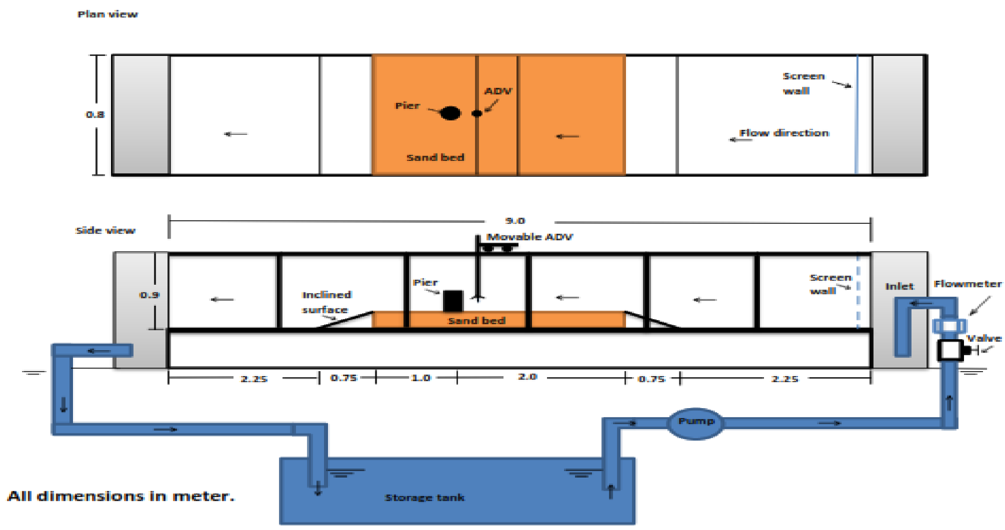

Figure 3.1 the Experimental flume (Ismael A. et al., 2015**).**

According to the experimental findings, the Sediment in the section had a specific gravity of 2.65 g/cm^3, a median particle size of 1.45 mm, a standard deviation of 3.16, and a median particle size of 3.16 mm. Based on Ettema's (1980) investigation, which found that as long as the ratio of pier diameter to grain size is greater than 50, the size of the bed soil's particles has little effect on scouring depth. Each pier used in the study met Ettema's requirements, having a ratio between 50 and 68 to consider the effect of sediment size on scour depth.

3.3 Numerical Methods

Several 3D numerical methods have successfully investigated local scour in a single circular pier after the first model done by Olsen and Melaanc (1993). However, a surprisingly large numerical gap remains in the local scour for irregular pier geometries. Another significant limitation is the computational time, which is significantly longer than required to complete a local scour test in an experimental investigation. However, as computer performance is expected to increase, more simulators can provide valuable information and have limitless potential. Flow-3D software, established by Flow Science Incorporation, was utilized to produce CFD modeling in this research project.

3.4 Data Preparation for Modeling Setup

This study will investigate the local scour around bridge pier in two models of piers to be used in the tests and will be used as reference models to compere the final results. The shape and dimensions of the tested models are shown in Figure 3.2.

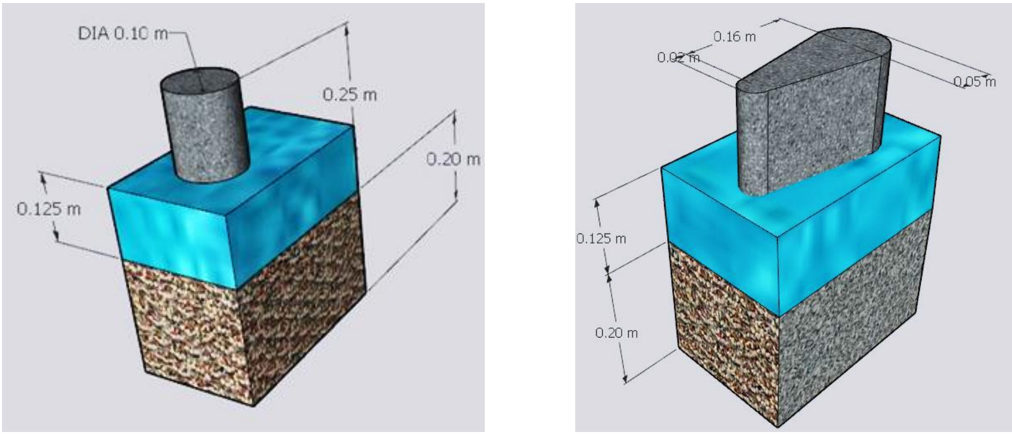

Figure 3.2 Dimensions of models.

The numerical model incorporated various data related to flow conditions, geometry, and sediment properties. To classify the soil material, the model utilized results from the mechanical sieve analysis and specific gravity test conducted as part of the study. The test results provided the following information:

Table 3.1 Flow conditions used in Flow-3D model.

Flow Conditions		**Geometry:**		**Sediment Properties**	
Discharge	0.058 m^3/sec	Pier Diameter:	0.1 m	Type t:	Sand
Water Depth	0.125 m	Pier Length:	0.45 m	Size of Sediment	1.45 mm
Velocity	0.58m/s	Flume Length	3 m	Specific Gravity	2.65 g/cm^3
		Flume Width	0.2 m	Sediment Layer	0.20 m

3.5 Scale Effect

Ismael investigation suggests that there are no scale effects arising from sediment characteristics, channel geometry, and flow conditions. The diameter of piers used in the Ismail study maintains a ratio between 50 and 68 with respect to the particle size. This choice aims to mitigate the influence of particle size on scour depth. Also, Based on Ettema's (1980) investigation, which found that if the ratio of pier diameter to particle size is greater than 50, the size of the bed particles has little effect on scouring depth.

3.6 Numerical Modeling

The numerical modeling in this study employed the robust computational fluid dynamics software known as Flow-3D, developed by Flow Science Incorporation. This software is widely recognized and utilized in various industries, including aerospace, automotive, and marine engineering, as well as in academia and research, due to its ability to simulate fluid flow, heat transfer, and related phenomena. Flow-3D utilizes a structured perpendicular grid approach using the fractional area volume (FAVOR) method, enabling the simulation of complex geometries. To accurately represent free surface flow, the Volume-Of-Fluid (VOF) method is employed, allowing for precise tracking of air, fluid, or fluid adjacent to fluid boundaries (Flow Science, 2008; Hirt and Nichols, 1981). This technique records the volume of fluid within each cell, disregarding the surrounding air, which results in distinct interfaces between flowing fluid and air without the need for fine meshes. The capability of Flow-3D in modeling local scour has been demonstrated in previous research, such as the study conducted by Brethour (2001), where the software incorporates the geometric characteristics of obstacles within the fluid domain through fractional face area and volume calculations.

In addition to its applications in research, Flow-3D is an ideal CFD software for use in the design phase of projects and for improving production processes. Its features and capabilities make it a valuable tool for simulating deposition, entrainment, bed load transfer, suspended load transport, and other related phenomena in fluid flow analysis.

3.7 Model Set-Up

Different pier geometry was used in this numerical study to simulate the local scour phenomenon. There are numerous steps involved in the software setup and configuration process. Users of Flow-3D have access to a variety of physical options, such as Sediment and scour, which call for the consideration of particular parameters. Gravity, viscosity, Turbulence, sediment parameters, and flow configurations are crucial parameters that must be set up to simulate Sediment scour. Gravity has been activated and needs to be set to -9.81 m/s^2. This sediment scouring model utilizes non-cohesive theories regarding Sediment and uses models of eroding processes advection, and deposition to estimate how the material moves. Table 3.2 shows how the sediment scours model expects various characteristics.

Table 3.2 Values of factors used in the Flow-3D model.

Factors	Value Estimate
Bed Roughness Ratio	1
Bedload Coefficient	8
Grain Size	1.45(mm)
Mass Density	2650(kg/cm3)
The Critical Packing Fraction	0.64
Critical Shields Parameter	0.05

The inlet boundary condition for the lower boundary in the Y direction (Y min) was specified as flow discharge, while the outlet boundary at the upper boundary (Y max), representing the end of the flume, was set as outflow. At the lower boundary (Z min) the bottom set as a wall boundary condition. Conversely, at the upper boundary (Z max) the pressure boundary condition was chosen to represent a free surface. For both (X min and X max) wall boundary conditions were selected to represent the channel sides, as showed in Figure 3.3. in all models used Three-dimensional mesh block with 50688 uniform cells.

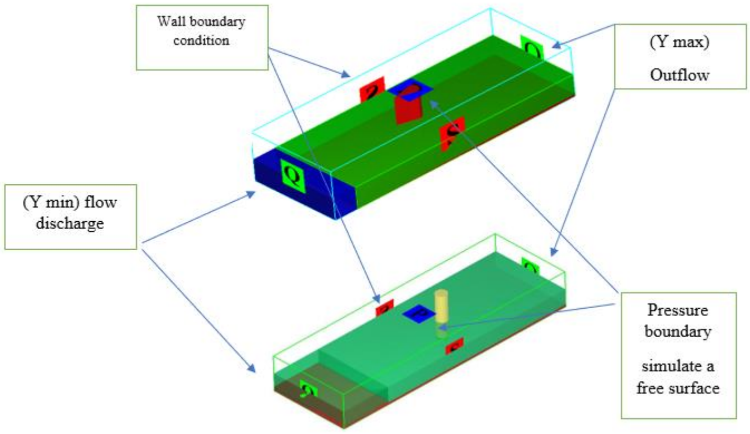

Figure 3.3 Boundary Condition.

3.8 Reliability of The Numerical Model

As shown in Figure 3.4, the models were validated to ensure the reliability of the numerical model. Validation process involved comparing the results obtained from the experimental and Computational Fluid Dynamics (CFD) analyses. A reference pier model was selected for each case, including a cylinder pier, as shown in Figures 3.4. The validation process involved a numerical simulation model in the same conditions of the laboratory investigation conducted by Ismael A. et al. (2015). The validation results provided valuable insights into the accuracy and validity of the numerical model of the circular pier by comparing the results of scour depth of the circular pier from the experimental study with the numerical model. This validation process helped establish the reliability of the numerical model and ensure its effectiveness in accurately representing the behavior of the studied pier configurations.

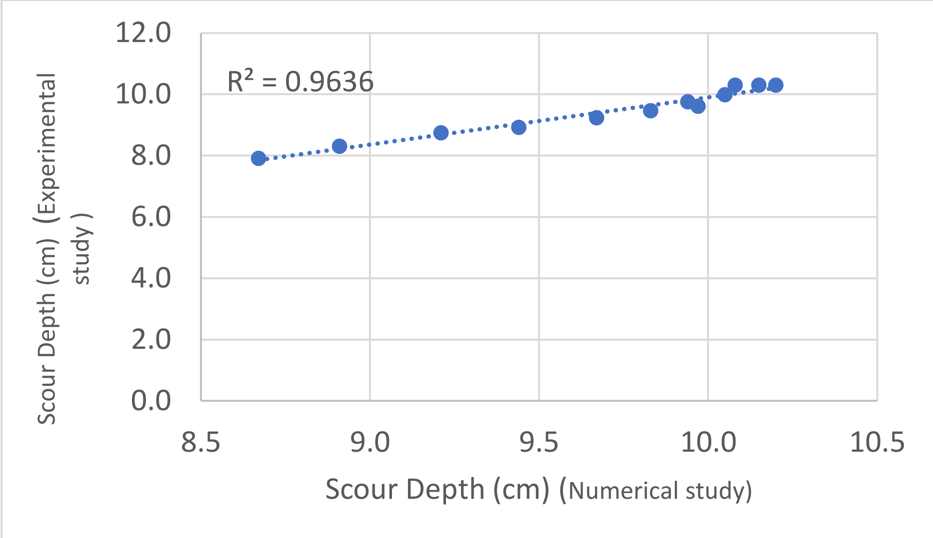

Figure 3.4 Validation of the Circular Pier Model.

Once the reliability of the numerical model has been established, the next step involves comparing the results obtained from Computational Fluid Dynamics (CFD). This model will serve as a basis for comparing the results obtained after implementing a collar countermeasure technique, specifically the use of a two collar to redirect the downward flow and minimize the impact of the horseshoe vortices. The selection of flow conditions, pier diameter, and sand size was influenced by the experimental study conducted by Ismael A. et al, (2015).

3.9 Model Definition for Pier and collar

The counter-measurement attachments for bed armour are essential for improving streamed resistance. These add-ons, which use collars or horizontal collars, are intended to enhance the pier's setup or equipment. One of the most efficient methods is the use of a Shape Pier with a collar, in which collars are placed in strategic contact with the piers to direct water flow away from them. The downflow is affected directly by the diameter and location of the collars, which lowers the depth of scouring. The collars completely cover the pier edges and are usually in contact with the pier's face to ensure effective protection as shown in Figures 3.5 and Figures 3.6. The collar, which is positioned at the natural bed level, effectively reverses and stops further scouring beyond its and the pier's depth. Although the collar's diameter significantly lowers scouring, its size is determined by practical factors. Furthermore, the use of plates helps to reduce the downflow on the pier's face, preventing the development of a horseshoe vortex.

The methodology aims to improve the pier's streamed resistance and safeguard it from the damaging effects of scouring by incorporating these bed armor counter measurement attachments and optimizing their design. After completing the validation process for the two reference pier models, namely a single-cylinder pier with a diameter of 10 cm and a nosed pier NP, the following analysis focused on three cases.

✓ Involved comparing the performance of a circular pier against NP.

✓ Involved comparing the performance of a circular pier against two models connected by a collar, where the collar diameter was two times and three times of the pier diameter as shown in Figure 3.5.

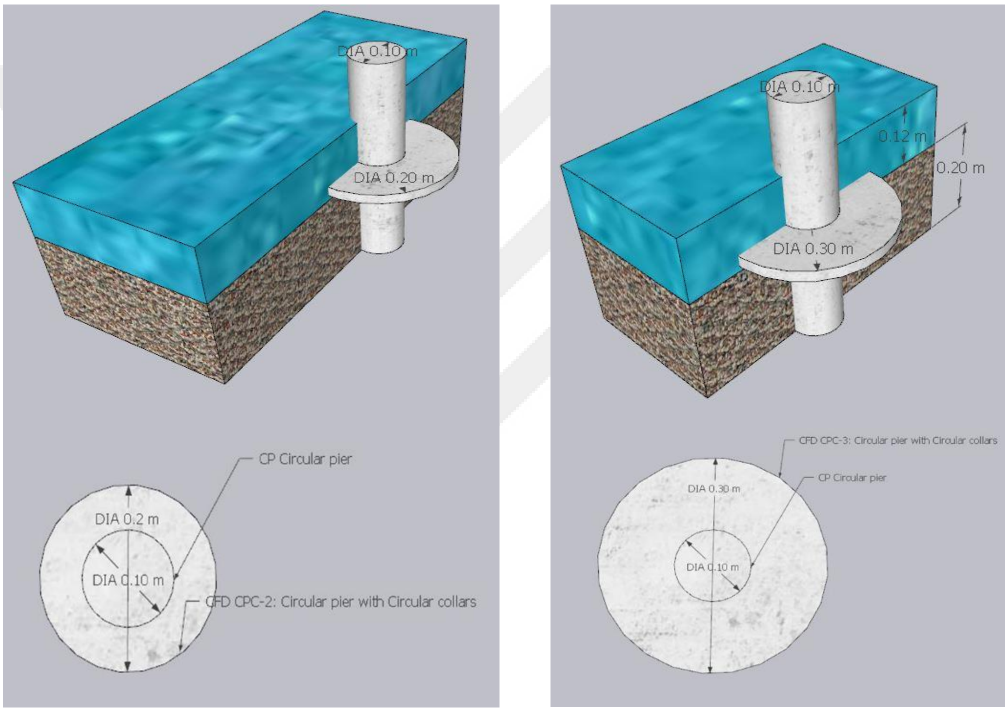

Figures 3.5 Pier connected by a collar diameter twice and three times that of the pier diameter.

✓ The analysis considered a downstream-facing circular pier NP attached each one of them connected by a collar, where the collar diameter was times and three times of the pier diameter in each case as appeared in Figure 3.6.

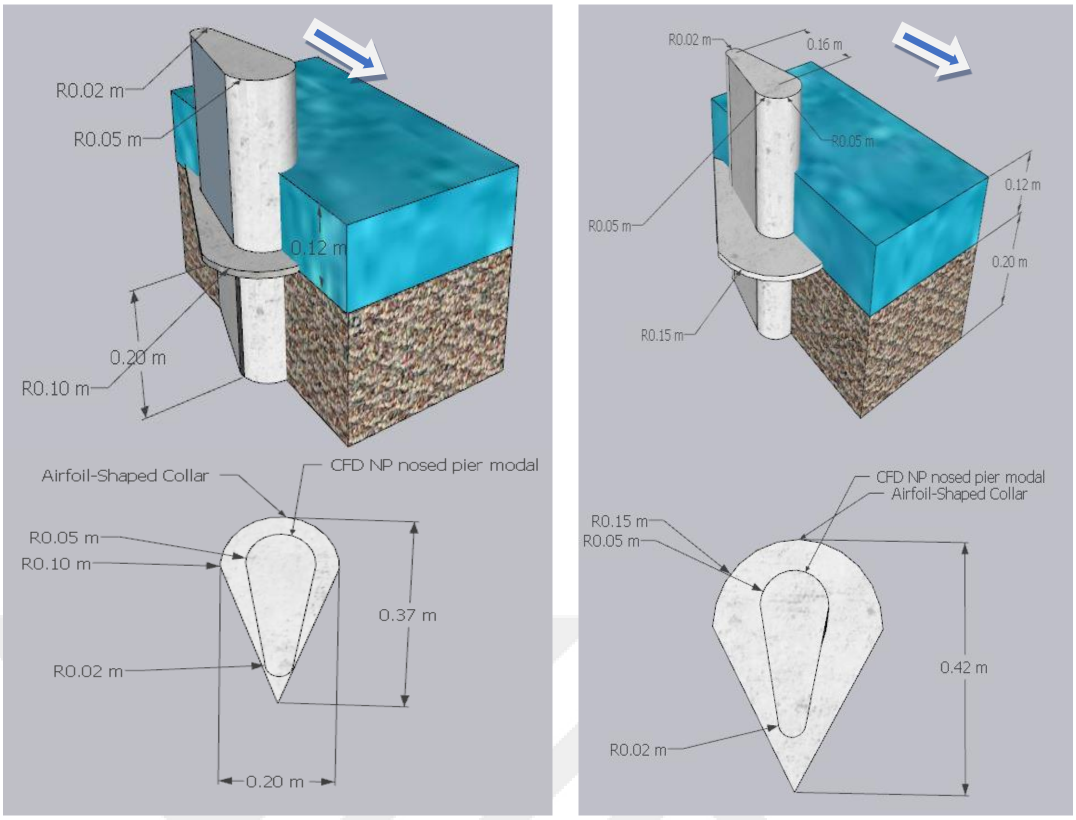

Figures 3.6 NP Attached to a collar.

The objective of these comparisons was to determine the optimal configuration for reducing the scouring effects.

3.10 Model Cases

The study includes six models, each involving a combination of two types of piers and two types of collars. The considered pier types are the circular pier and the nose-shaped pier, while the collar types consist of the circular collar and the airfoil-shaped collar. For each collar configuration, there are two collar diameters. In detail, the six cases can be summarized as follows:

1) **(CP):** Numerical reference circular pier model – This model serves as the reference and represents a simple circular pier without collars. The conditions for this model are based on an experimental study conducted by Ismael A. et al. et al. (2015).
2) **(CPC-2):** Numerical Circular pier with collars at the bed sediment two times the pier diameter – In this model, collars are placed at the bed sediment around the circular pier, and the collar diameter is twice the diameter of the pier.

3) **(CPC-3):** Numerical Circular pier with collars at the bed sediment three times the pier diameter – Similar to the (CPC-2) model, this configuration involves collars at the bed sediment, but the collar diameter is three times the diameter of the pier.
4) **NP:** Numerical Nosed pier model – This model represents a nosed pier shape without collars.
5) **(NPC-2):** Numerical nosed pier model with airfoil-shaped collar two times the nosed pier diameter – in this model, the nosed pier configuration is combined with collars placed at the bed sediment, with the collar length being two times the diameter of the nosed pier.
6) **(NPC-3):** Numerical nosed Pier Model with Airfoil-Shaped Collar Three Times the Nosed Pier Diameter – Similar to the (NPC-2) model, this configuration involves collars placed at the bed sediment around the nosed pier, but the collar length is three times the diameter of the nosed pier.

The models will be divided to compered as following:

In the first case

1. Comparison of Experimental Results with a Numerical Reference Circular Pier Model (CP).
2. Comparing the results of the numerical circular pier model (CP) with the Collars Two Times the Pier Diameter (CPC-2) model.
3. Comparing the results of the numerical circular pier model (CP) with the Collars Two Times the Pier Diameter (CPC-3) model.

In the second case

1. Comparing the results of numerical nosed pier model NP with Circular Pier Model (CP).
2. Comparing the results of numerical nosed pier model NP nosed pier model with airfoil-shaped collar (NPC-2) model.
3. Comparing the results of numerical nosed pier model NP nosed pier model with airfoil-shaped collar (NPC-3) model.

CHAPTER 4
RESULTS AND DISCUSSION

4.1 Introduction

Determining the depth of scouring surrounding bridge piers is an important part of the initial design stage because it affects the choice of bridge pier type. As a result, the depth of scouring is the most significant variable in the bridge pier design process. The findings of a numerical simulation study carried out using FLOW-3D software to investigate the scour phenomenon around two different kinds of bridge piers namely circular pier (CP) and nosed pier (NP). To reduce scouring, a countermeasure method known as the collar with two different diameters (2D and 3D, where D stands for the bridge pier diameter) was used. By creating contact and support within the pier structure, the collar acts as the primary approach to reducing scouring surrounding the bridge pier. The results of our numerical simulations are presented throughout this chapter, providing valuable insights into the scouring behavior around these bridge pier types and the effectiveness of the collar as a countermeasure.

4.2 Model cases

In this study, six models in three cases were considered to investigate the reduction of local scour depth by using collars as follows.

First case for:

1- The results of experimental model with numerical reference circular pier model symbolize it as (CP)

2- The results of numerical circular pier model (cp) attached to collars two times the pier diameter symbolizes it as (CPC-2).

3- The results of circular pier model (cp) attached collars three times the pier diameter symbolize it as (CPC-3)

The Second Case

1. The results of numerical nosed pier model symbolize it as np attached numerical circular pier model (CP)
2. The results of numerical nosed pier model NP nosed pier model attached airfoil-shaped collar symbolize it as (NPC-2). two time of the pier up stream diameter.
3. The results of numerical nosed pier model np nosed pier model attached airfoil-shaped collar symbolize it as (NPC-3). three time of the pier up stream diameter.

4.3 Results for First case

4.3.1 Circular Pier (CP) without collar

Results were remarkably consistent of the experimental and computational models for the single circular pier without any collar attachments. The physical test produced result of the maximum scour depth was 10.2 cm whereas the maximum scour depth predicted by the numerical model for the circular pier was 10 cm as shown in Figure 4.1 Scour profile around circular pier model (CP). The local scour phenomenon around the pier is highlighted by the color gradient on the canal bed, which shows the scour depth levels of the bed silt. The key bar's variation in color determines how much the scour level changes and it represents as in all models.

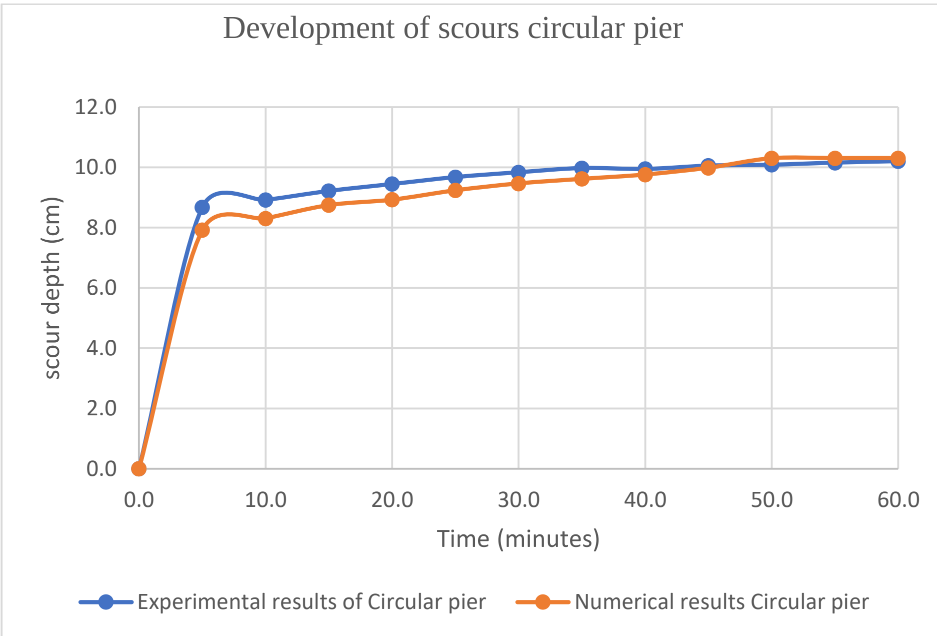

Figure 4.1 Development scours between (CP) and experimental model.

Furthermore, significant similarities were observed between the Experimental Circular Pier and the numerical circular pier when analyzing the evolution of scour depth over time, as depicted in Figure 4.1. The accuracy of the circular pier's model was established through the determination of the maximum scour depth within this model, highlighting its utility as a reference for comparison in all subsequent models. Figures 4.2 and 4.3 illustrate the scour profile and the two-dimensional velocity vectors of the water flow field around the Circular Pier Model (CP). The flow of water generates vortices around circular piers, leading to concentrated erosion on the pier's bed surface. Consequently, scour holes develop on the sides of the pier that are exposed to the flow, with the most significant scour depth occurring on the lateral sides on the upstream face.

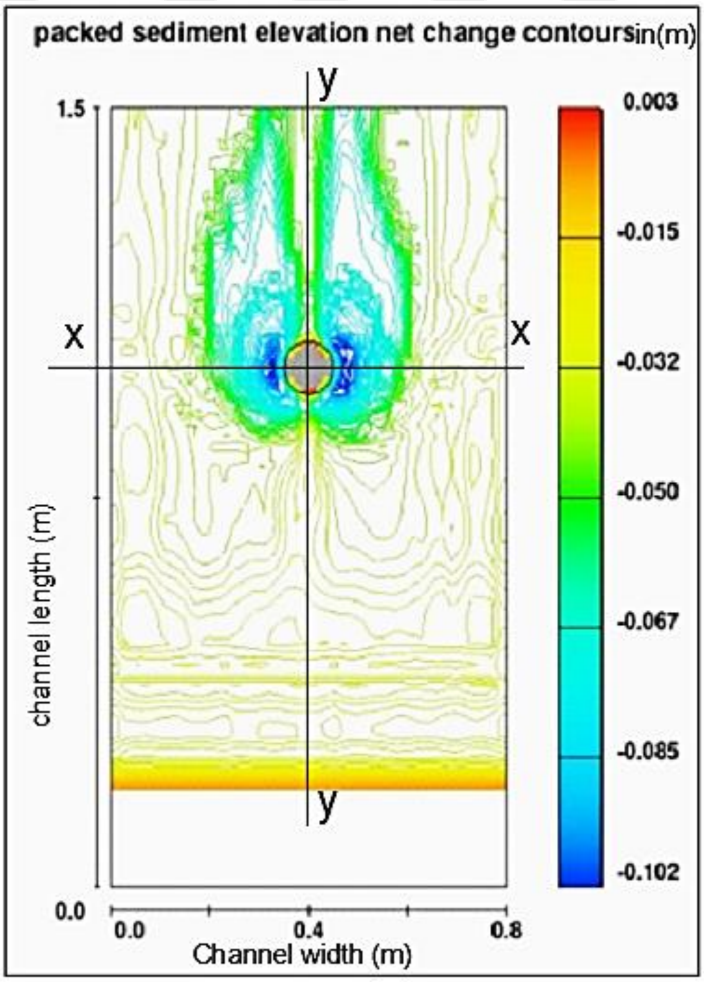

Figure 4.2 Scour profile around circular pier model (CP)

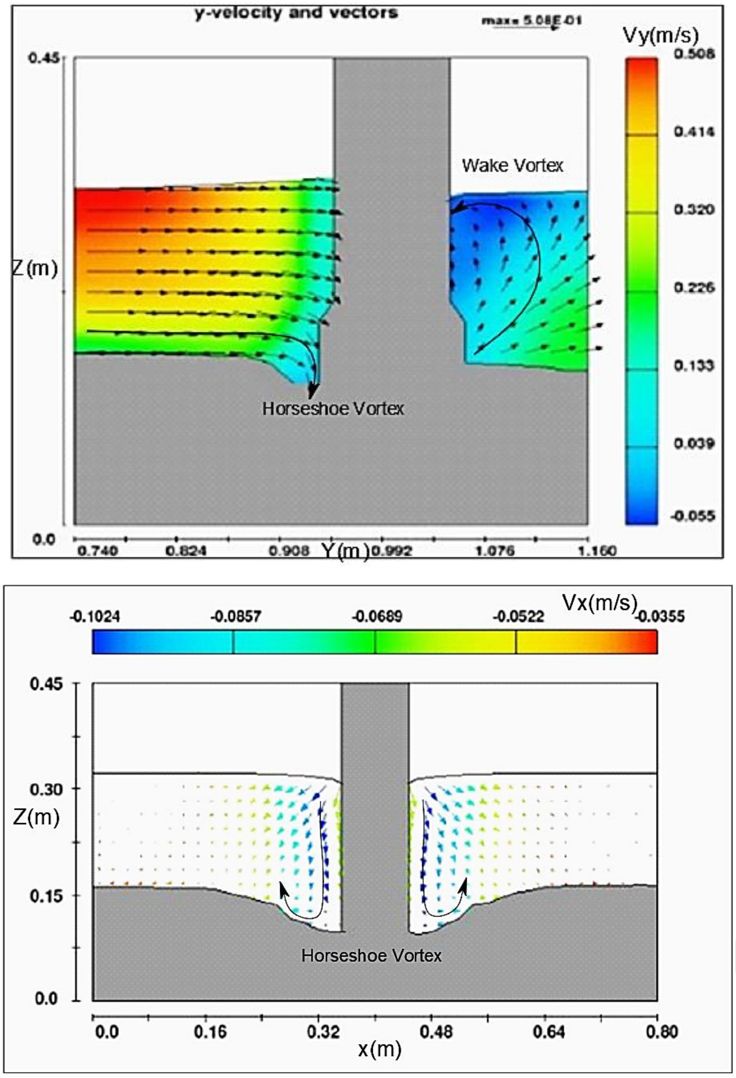

Figure 4.3 Two-dimensional velocity vectors and the water flow field around the circular pier model

4.3.2 (CP) with (CPC-2) Results

When comparing the reference circular pier (CP) with the circular pier attached to collar (CPC-2) a notable decrease in scour depth was seen. The maximum scour depth estimated by the computational model for the single circular pier without any attachments was 10.3 cm. The scour depth was decreased to 7.6 cm when the collar with two time of bridge pier added as shown in Figure 4.4 and Figure 4.5. The reduction percentage was about 26.3%. This outcome illustrates that the (CPC-2) works as a preventative measure to minimize scouring around the bridge pier.

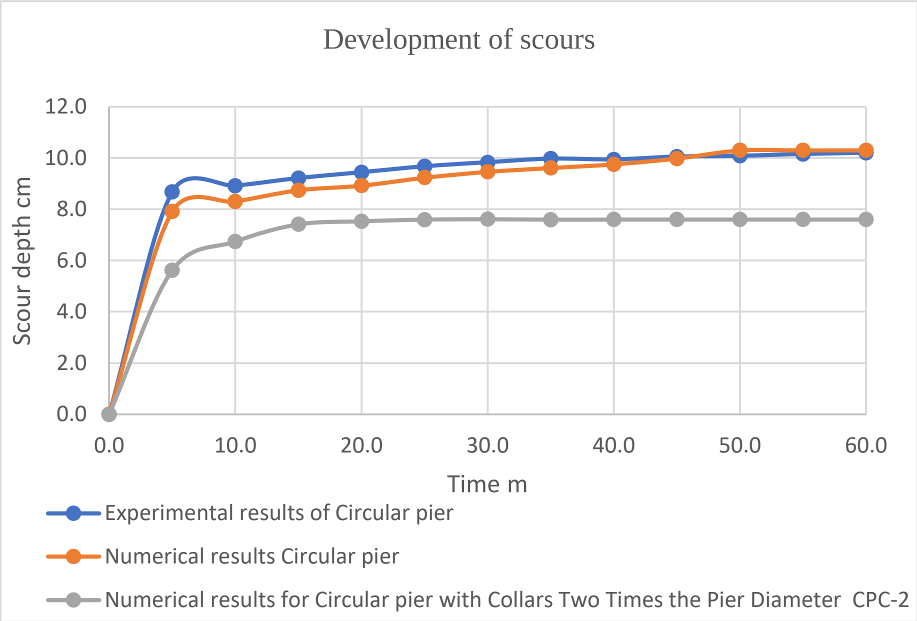

Figure 4.4 Development scours for (CP) and (CPC-2).

Figure 4.5 shows the scour profile around the circular pier (CPC-2 and Figures 4.6 shows scour profile with two-dimensional velocity vectors and the water flow field around the Circular Pier Model with collar (CPC-2).

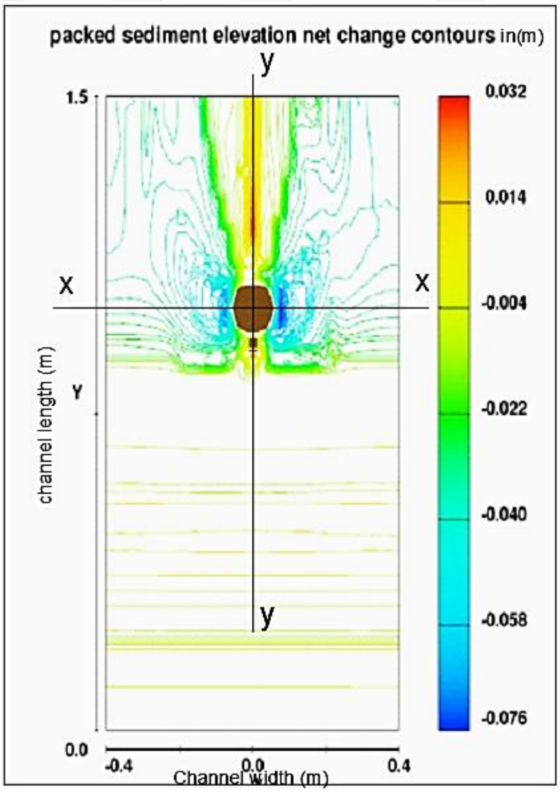

Figure 4.5 Scour profile around circular pier model (CPC-2)

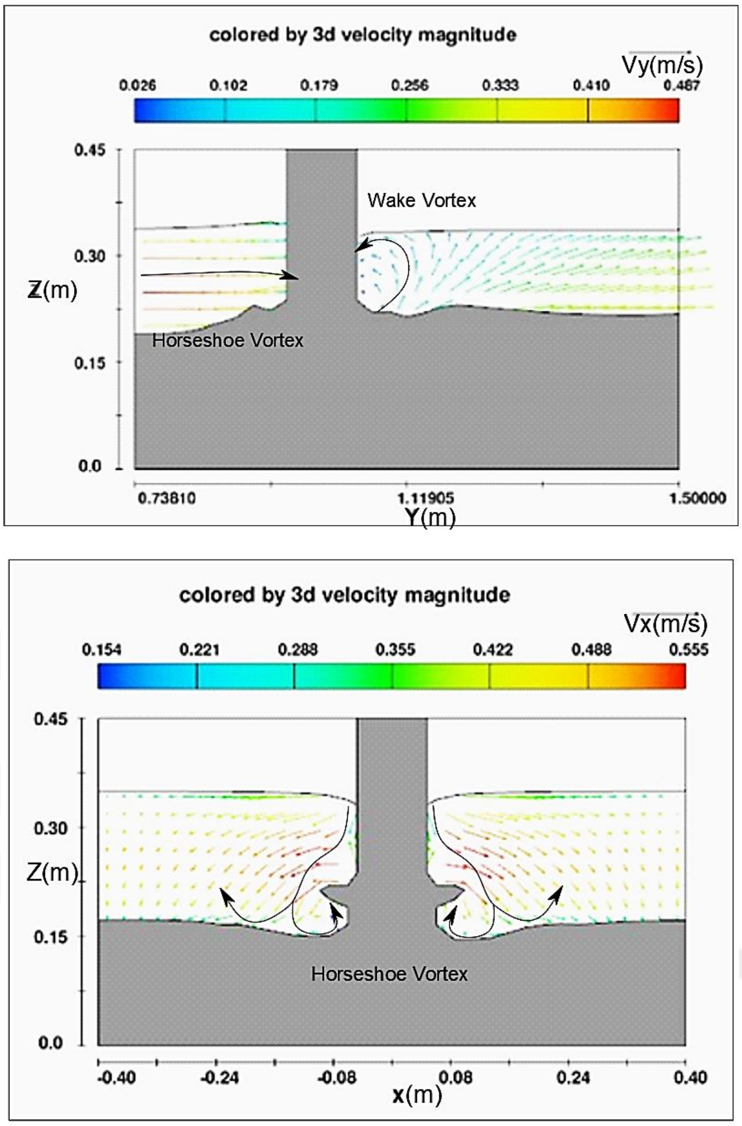

Figure 4.6 Two-dimensional velocity vectors and the water flow field around the circular pier model with collar (CPC-2)

4.3.3 Comparison of (CP) with (CPC-3) Results

When comparing the reference circular pier (CP) to the Circular pier attached to a collar in (CPC-3) model, an important decrease in scour depth was observed. The computational model for the single circular pier without any attachments (CP) resulted in a maximum scour depth of 10.3 cm. However, the model of (CPC-3) as shown in Figure 4.7, the scour depth significantly decreased to 5.9 cm, representing a reduction percentage of 43%.

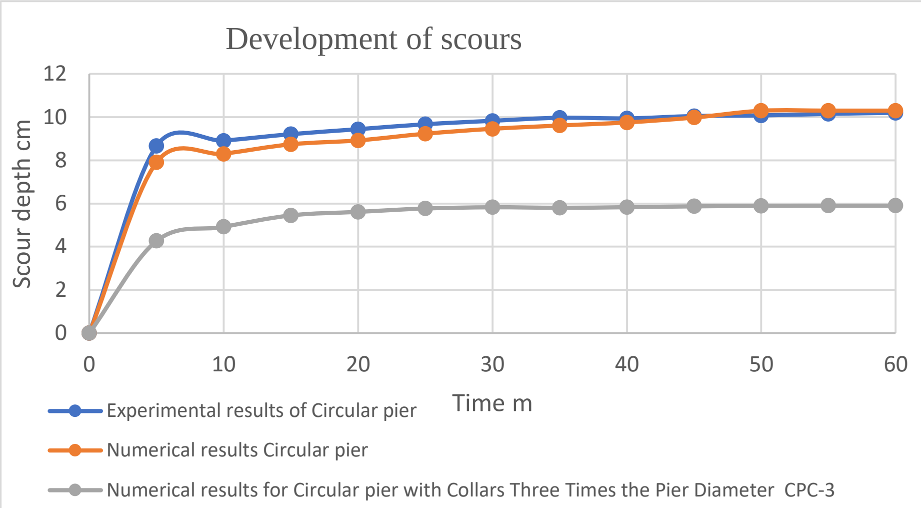

Figure 4.7 Development scours between (CP) and (CPC-3).

Figure 4.8 show the scour profile two-dimensional velocity vectors and the water flow field around the Circular Pier Model (CPC-3) and Figures 4.9 show scour profile two-dimensional velocity vectors and the water flow field around the Circular Pier Model with collar (CPC-3)

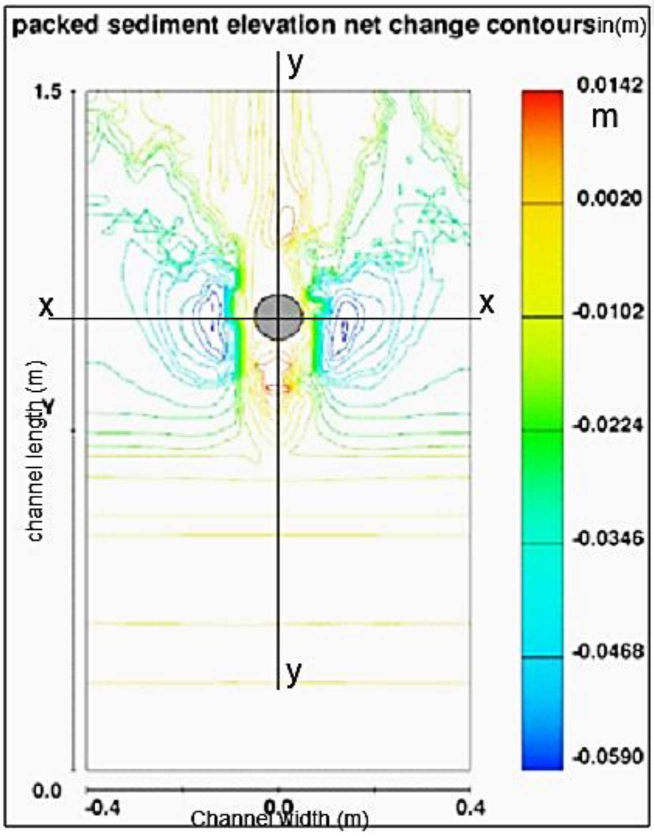

Figure 4.8 Scour profile around circular pier model (CPC-3)

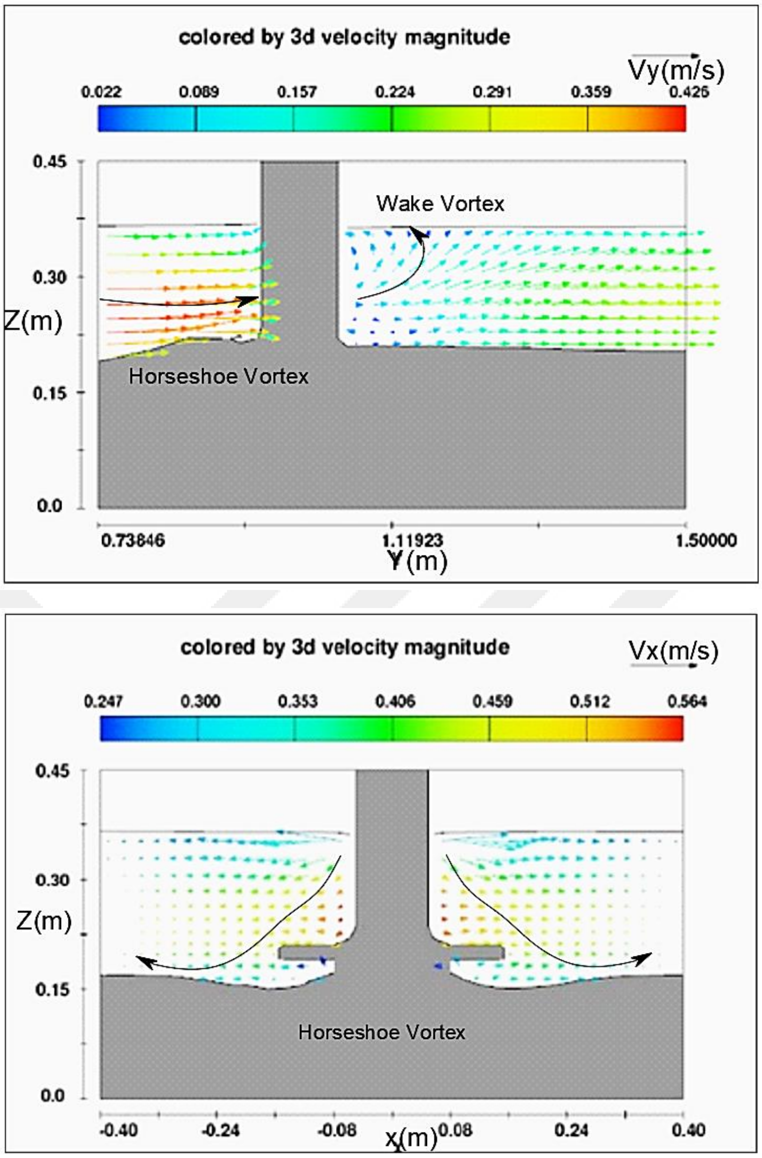

Figure 4.9 Two-dimensional velocity vectors and the water flow field around the circular pier model with collar (CPC-3).

The mechanism of the collar utilizes its strategic positioning and geometry. The collar effectively creates a barrier that alters water flow patterns, minimizing the scouring effect, by surrounding the pier in three dimensions.

The (CPC-3), acts as a protection against the erosive action of flowing water, reducing the scouring around the bridge pier by providing contact and content within the pier structure. When comparing the (CP) with the (CPC-2) and (CPC-3) models, this result highlights the effectiveness of the (CPC-3) model as an effective countermeasure to enhance the stability and longevity of bridge piers against scour phenomena.

4.4 Results for Second Case

4.4.1 Numerical Nosed Pier Model NP

The findings for numerical nosed pier model NP with the experimental study nosed pier model will compare. Also, the results of numerical nosed pier model NP will compare with nosed pier model attached to airfoil-shaped collar (NPC-2) model then with nosed pier model attached to airfoil-shaped collar (NPC-3) model.

4.4.2 Comparison of NP with Experimental Nosed Pier Results

The results of the comparison between the experimental nosed pier model and numerical nosed pier model NP showed remarkable reliability. The scour depths for the experimental pier model without any attachments were closely in both experimental and computational models. Calculated value of the scour depth in the experimental test was 4.9 cm, while the CFD model predicted a maximum scour depth of 4.10 cm as shown in figure 4.11. The changing of scour at the canal bed effectively highlighted the local scour phenomenon around the nosed pier, revealing the changing levels of bed sediment. The color variation of the key bar served as a visual indicator of scour level changes.

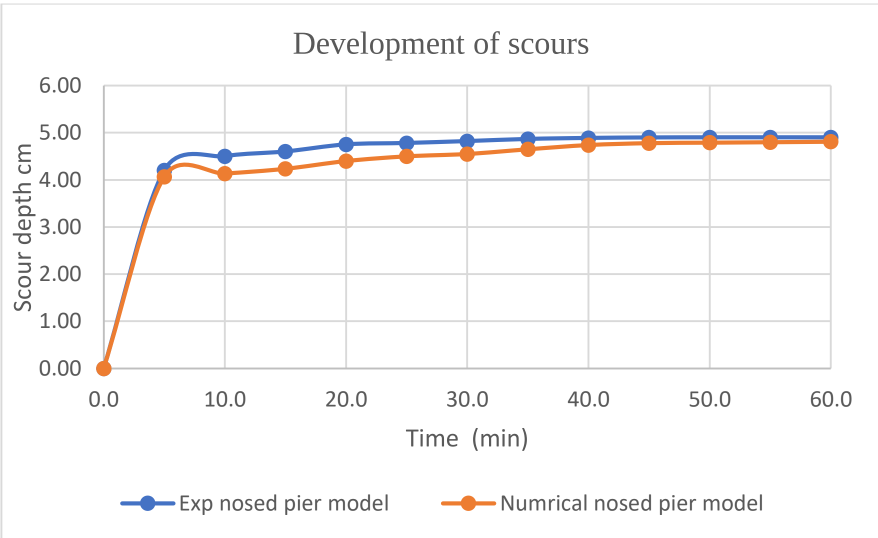

Figure 4.10 Development scours between NP and Experimental Nosid Pier.

Figure 4.11 show the scour profile two-dimensional velocity vectors and the water flow field around the nosed pier model NP and Figures 4.12 show scour profile two-dimensional velocity vectors and the water flow field around the nosed pier model NP.

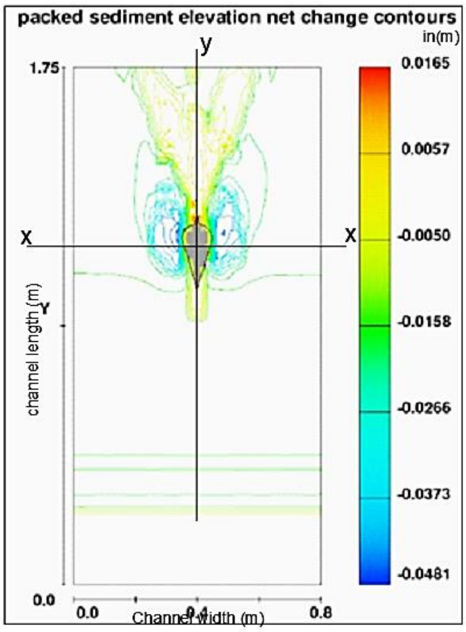

Figure 4.11 Scour profile around nosed bridge pier model NP

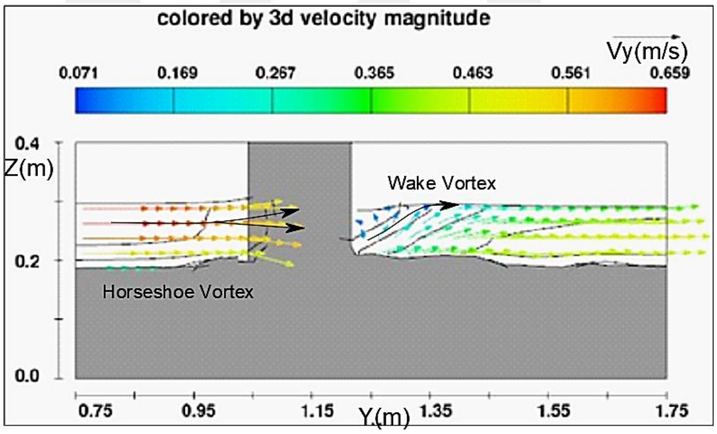

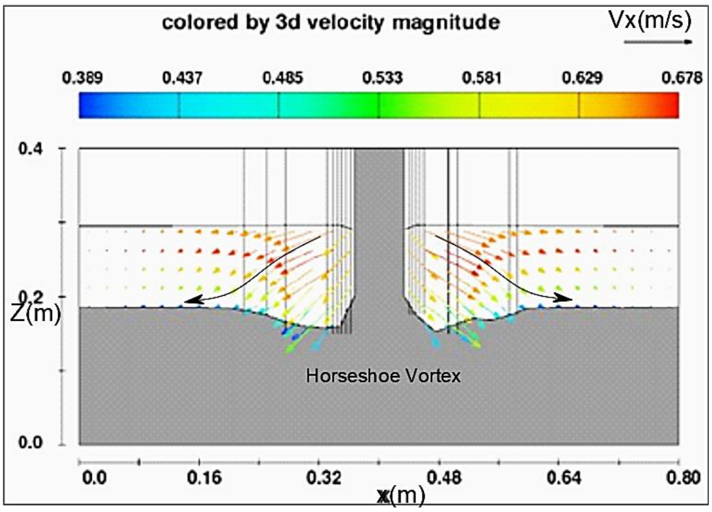

Figure 4.12 Two-dimensional velocity vectors and the water flow field around the bridge pier model NP

4.4.3 Comparison of NP with (NPC-2) Results

A significant reduction in scour depth was observed when comparing scours depth around nosed bridge pier model NP with the nosed pier modal NP attached to airfoil-shaped collar (NPC-2). Results of the maximum scour depth of the nosed pier modal NP without any attachments was 4.81 cm. But, adding airfoil-shaped collar in (NPC-2) model gives a significant decrease of about 3.0 cm. This reduction in scour depth to 18.4% reduction in percentage as shown in Figure 4.13.

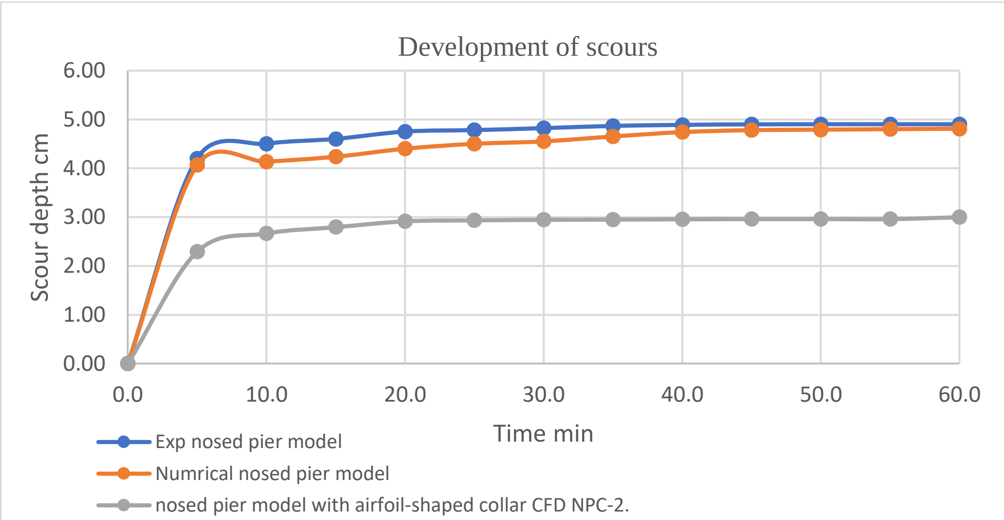

Figure 4.13 Development scours between (NPC-2) and Experimental Nosed Pier.

The application of the nosed pier model with airfoil-shaped collar (NPC-2). It demonstrates its effectiveness as a scouring mitigation measure around the nosed pier model NP. The collar redirect water flow and reduces the erosive impact of flowing water by providing contact and content within the pier structure, resulting in improved pier stability. Figures 4.14 and 4.15 shown the scour profile also, the velocity vectors and the water flow field around the nosed pier model with airfoil-shaped collar CFD (NPC-2) and

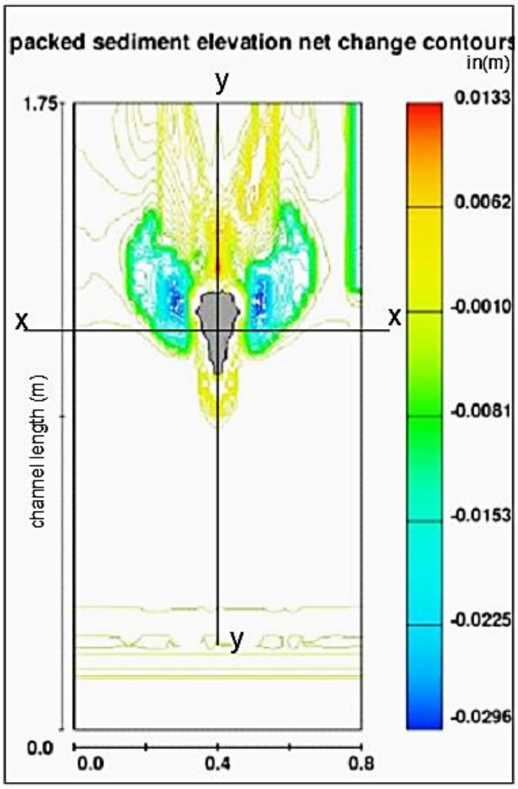

Figure 4.14 Scour profile around the nosed bridge pier model with airfoil-shaped collar (NPC-2)

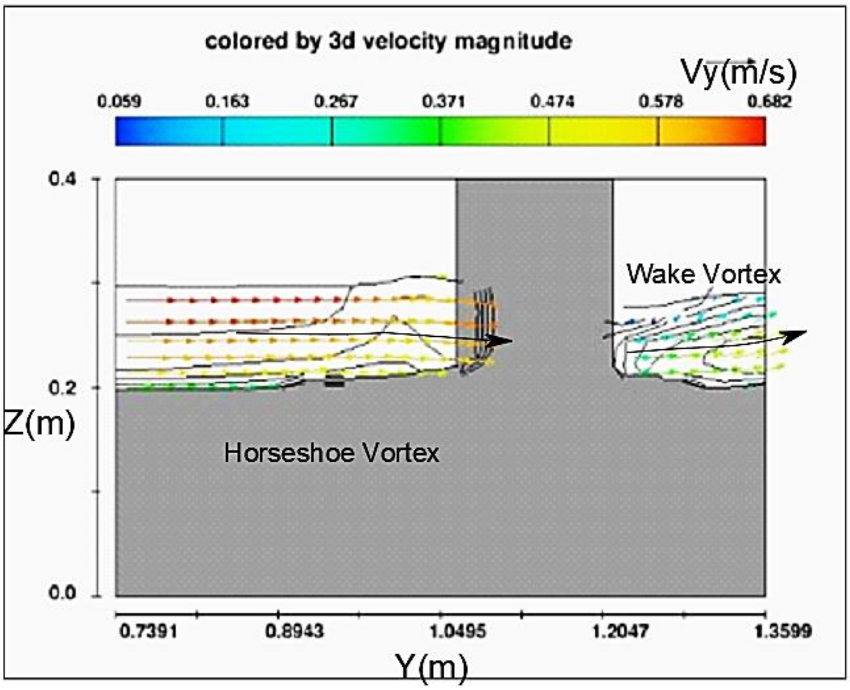

Figure 4.15 Two-dimensional velocity vectors around the nosed bridge pier model with airfoil-shaped collar (NPC-2)

4.4.4 Comparison of NP with (NPC-3) Results

A significant decrease in scour depth was detected with the nosed pier with collar (NPC-2). The numerical nosed pier model NP produced a maximum scour depth of 4.81 cm without any attachments.

However, by adding the nosed pier with collar (NPC-2), a significant decrease of the maximum scour depth near 2.7 cm. When the maximum scour depth in nosed pier model was reduced to 4 cm, the percentage of reduction in scour depth equates to a 43.8 % as Illustrated in Figure 4.16.

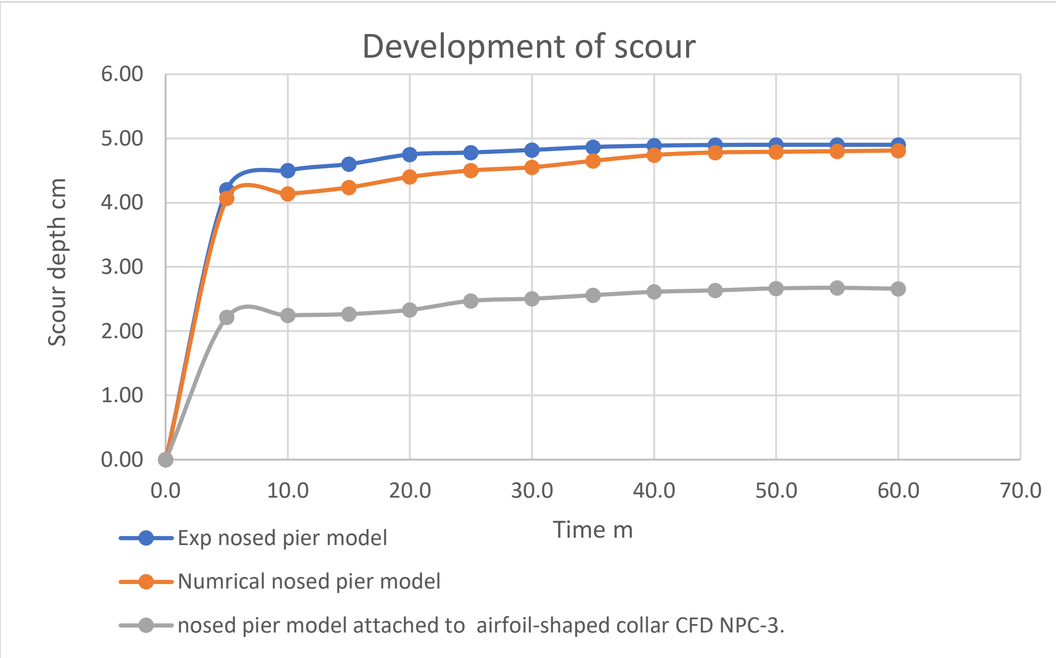

Figure 4.16 Development of scours between (NPC-3) and Experimental Nosed Pier NP.

The use of the nosed pier model with the airfoil-shaped collar (NPC-3). It proves its efficacy as a scouring mitigation method in the vicinity of the nosed pier model NP, the collar redirects water flow and lessens the erosive influence of flowing water, resulting in increased pier stability. Figure 4.17 and Figure 4.18 depicts the scour profile, velocity vectors, and water flow field around the nosed pier model with airfoil-shaped collar (NPC-3).

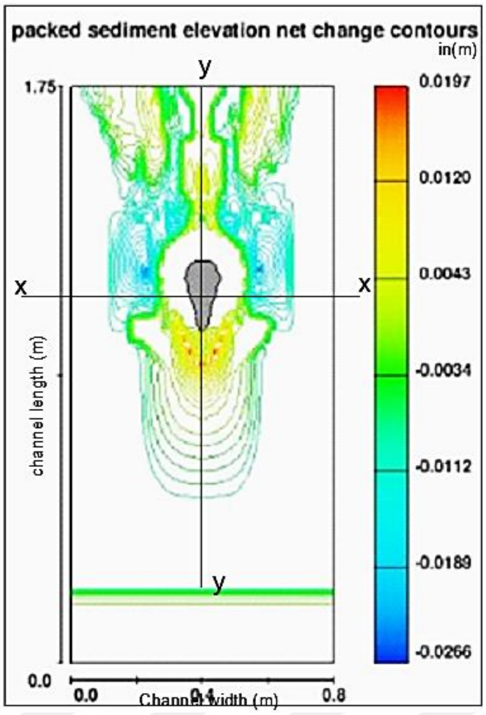

Figure 4.17 Scour profile around the nosed bridge pier model with airfoil-shaped collar (NPC-3)

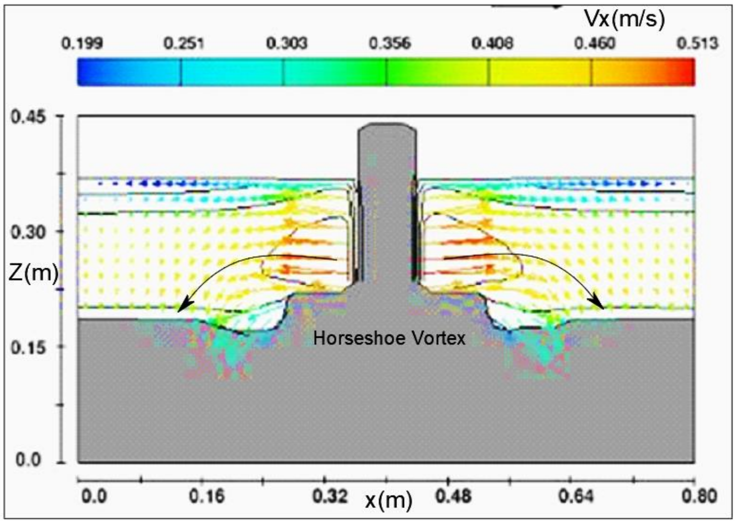

Figure 4.18 Two-dimensional velocity vectors and the water flow field around the nosed bridge pier model with airfoil-shaped collar (NPC-3).

4.5 Flow Field and Scour Mechanisms Around Bridge Pier

4.5.1 Flow Field Around Bridge Pier

The presence of the pier within the canal introduces a hydraulic obstruction that significantly influences the water flow dynamics. Upstream of the pier, the flow maintains a uniform velocity of approximately 0.58 m/s. However, as the flow encounters the pier, distinct changes in flow patterns become apparent in all cases, upon reaching both sides of the pier, the velocity of the water notably increases. signifying the accelerated flow in these regions. Notably, within the scour hole formed downstream of the pier, the flow dynamics exhibit intriguing behavior. Illustrated by the dark blue vectors in the opposite direction, a flow reversion phenomenon takes place on the rear side of the pier as shown in Figures 4.19, 4.20, 4.21, 4.22. where the flow vectors appear to be pointing inwards towards the scour hole. This flow reversion leads to the creation of a vortex within the scour hole, initiated at the bottom of the pier due to the downward flow.

4. 5. 2 The Mechanics of the Scour Around the Circular Bridge Pier

The circular bridge pier is more exposed to local scouring phenomena due to their symmetrical shape on the surfaces. Water flow around circular pier creates vortexes, leading to concentrated erosion on the pier surface. As an outcome, scour holes tend to develop on the sides of the pier facing the flow, with the scour depth occurring on the front and the maximum scour depth occurring on lateral side on the upstream side. The flow pattern in the surroundings of a circular bridge pier undergoes a transition to a dynamic and intricate state as a scour hole takes shape around the pier, the mechanism of this can be described from the figure 4. 19. As the water approaches the circular pier, it flows smoothly around its circular shape. However, the decrease in flow velocity from the surface of the water to the bottom creates a pressure gradient on the upstream side of the pier as shown Figure 4.19 (A1, A2). This pressure difference forces the water downward along the pavement face as shown in Figure 4.19 (A2) as a result of a decrease in flow speed from the surface to the bed leads to a reduction in stagnation pressure on the pier's face, creating a downward flow gradient, with the incoming flow, resulting in the formation of a complex vortex formatting called horseshoe vortices as shown in Figure 4.19 (A3). As a result of the continuity of the incoming flow horseshoe vortices extend to both sides allowing for an extension of the scour holes around the bridge pier Figure 4.19 (A4).

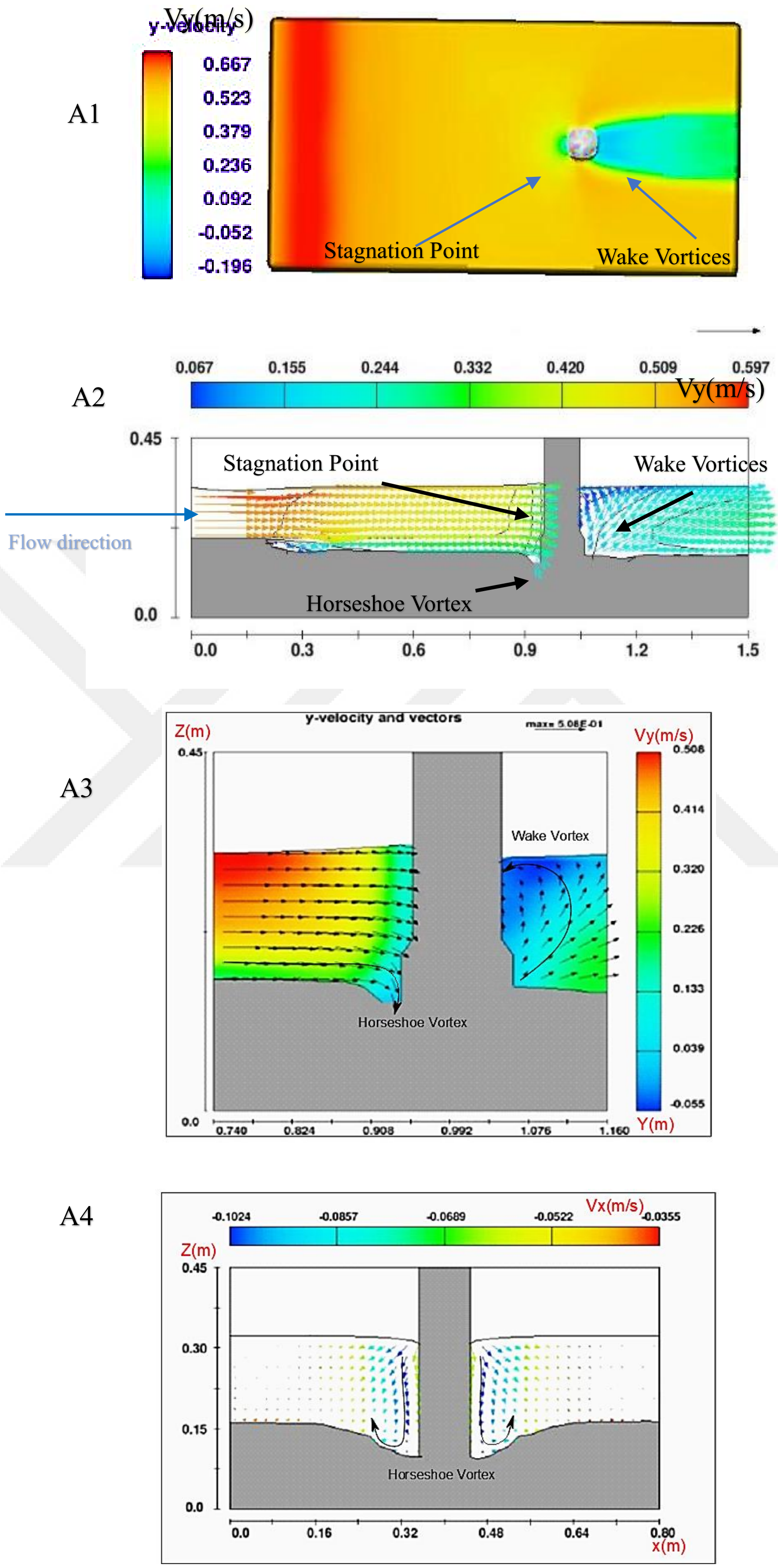

Figure 4.19 Flow field and velocity vectors around the bridge pier model (CP).

4. 5. 3 The Mechanics of Vortices Around Nosed Bridge Pier

Nosed bridge piers NP display distinct scour mechanisms when compared to circular piers due to their unique narrowing shape. This nosed design enables smoother water flow around the pier, which in turn reduces the formation of vortices and minimizes scouring. As water flows downstream along the rounded nose of the NP, the pier's configuration encourages gradual energy dissipation, resulting in less concentrated erosion as shown in Figure 4. 20 (B1).

Generally, NP models experience lower scour depths in contrast to circular piers, particularly on their lateral sides facing the flow. The most significant scour depth is typically found on the sides where water forces are at their highest. In other word, the mechanism of vortices around a nosed bridge pier is similar to that around a circular bridge pier, but the pier's shape directly influences the dynamics. In the case of NP, the pier's shape gradually tapers from the front face opposite the upstream flow, affecting the velocity of water flow around it as shown in Figure 4. 20 (B2).

Because of the reduced width of the pier at the front face, the formation of vortices is constrained in this region. As water approaches the pier, the vortices spread and extend along the sides, increasing in intensity as the width widens towards the edges of the pier. This process entrains sediments, leading to the development of a scour hole around the nosed bridge pier as shown in Figure 4. 20 (B2) and (B3).

B1

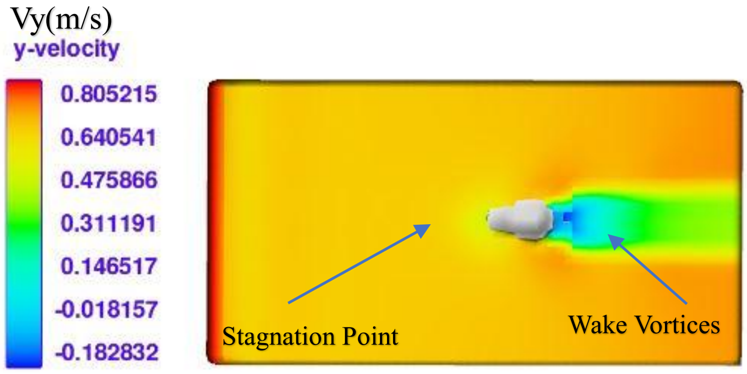

B2

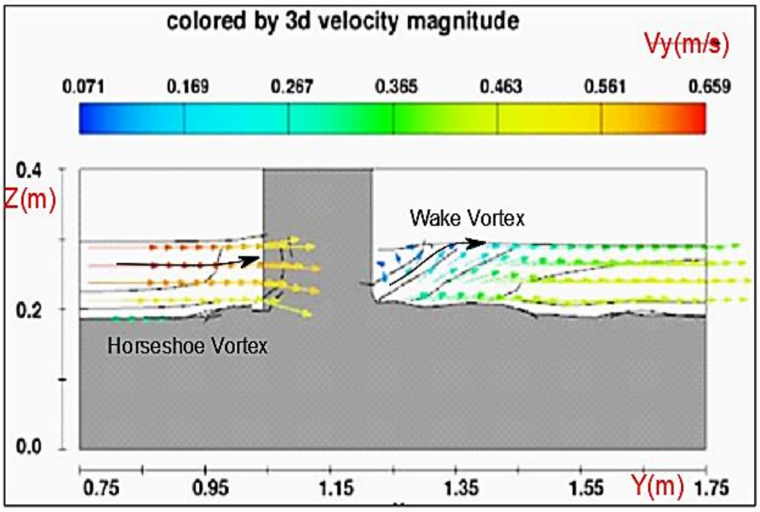

B3

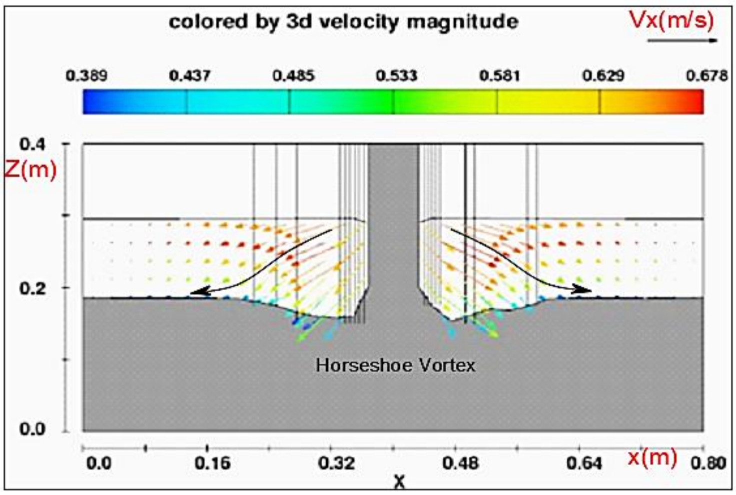

Figure 4. 20 Flow field and velocity vectors around the bridge pier model NP.

Circular piers tend to generate more balanced and uniform horseshoe vortices due to their uniform shape. In contrast, nosed piers with tapered fronts exhibit distinct vortex patterns influenced by the gradual increase in pier width, leading to more complex flow dynamics and less scour depth.

4. 5.3 The mechanics of the vortices around the bridge pier with collars

Collars are attached to bridge piers with the aim of reducing the formation of vortices and reducing scour depth around the pier. They can be particularly effective when used in combination with circular bridge piers and nosed piers. Two types of collars were used in this study namely airfoil-shaped collar and circular collar. As shown in the figure collar converts the flow patterns around the pier by controlling the flow of water near the bed of sediments, also, it was noticed that redirecting and redistributing the flow in a way that reduces the formation of vortices as shown in Figure 4. 21 (C1) and (C1). By disrupting the flow patterns that typically show vortex formation, collars help minimize the intensity and extent of these vortices.

Collars can disrupt the shedding of vortices, which in turn reduces the entrainment of sediments and erosion. By breaking up the vortices, collars can limit their erosive impact on the surrounding bed. also, collars divert and disperse the flow of water as it approaches the bridge pier as shown in Figure 4. 21 (C1) and (C1). This flow divergence helps in dissipating the energy of the flowing water gradually. As the energy is dissipated more evenly and less forcefully, the scouring effect on the riverbed is reduced.

In addition, this method has strategically positioned to protect the most vulnerable areas of the bridge pier where scour is most likely to occur. By shielding these areas from the direct impact of the flowing water, they help minimize scour depth and protect the pier's foundation. The collar attached to the bridge pier plays a crucial role in reducing vortex strings and scour depth. They achieve this by controlling flow patterns, disrupting vortex shedding, diverting and dispersing water flow, and protecting vulnerable areas of the pier. By mitigating these scour-related factors, collars enhance the longevity and safety of bridge structures in river environments.

C1

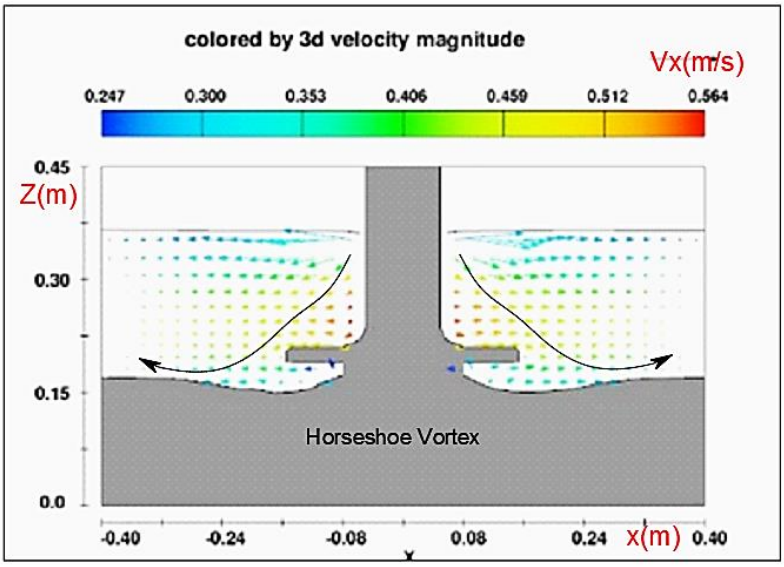

Figure 4.21 Flow field and velocity vectors around the bridge pier model (CPC-3).

C2

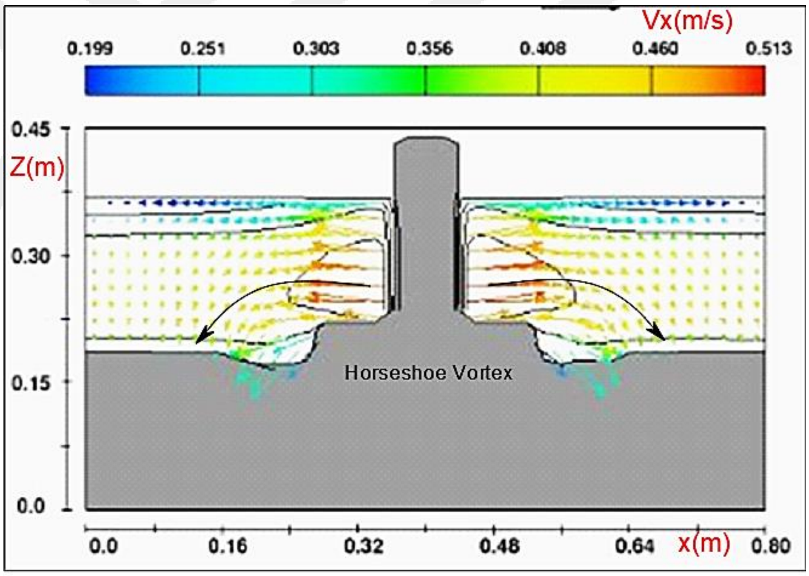

Figure 4.22 Flow field and velocity vectors around the bridge pier model (NPC-3).

When comparing the scour mechanisms between circular piers and nosed piers model NP, some key differences emerge. Circular piers are more prone to localized scouring due to their symmetrical shape, leading to more pronounced scour holes on their lateral sides facing the flow. On the other hand, NP models experience less localized scouring, with smoother water flow and reduced vortices due to their design. The effectiveness of countermeasures such as collars can further influence the scour mechanisms for both types of piers. Collars act as barriers, disrupting flow patterns and reducing scour depth around the pier. Their application can alter the scour mechanisms and enhance the stability of bridge piers in both NP designs.

The dynamics of horseshoe vortices and their impact on scour depth around bridge piers, whether circular or nosed, are influenced by various factors, including pier shape, flow velocity, and turbulence.

4.6 Over All Discussion

This section provides a discussion that includes the results of all the samples examined and presents the simulation results' overarching conclusions and their implications for bridge pier design and scour reduction.

In the first case, compared the results of two models for circular piers attached to collar at the bed sediment: (CPC-2) (collars two times the pier diameter) and (CPC-3) (collars at three times the pier diameter) against the Reference Model (CP) representing as the reference model of a circular pier without any collar. The (CP) exhibited a maximum scour depth of 10.3 cm, serving as a baseline for comparison. when the of collar was attached, significant reductions in scour depth were achieved. The (CPC-2) model resulted in a maximum scour depth of 7.6 cm, representing a reduction of 26.3% compared to the (CP). Additionally, the (CPC-3) model produced a maximum scour depth of 5.9 cm, showcasing an even more substantial reduction of 42.7% compared to the (CP). These findings underline collars' effectiveness in mitigating scouring around circular piers, the oversized collars providing more significant scour depth reduction as display in Figure 23.

The first case results demonstrate collar effectiveness in reducing scour depth around circular piers. The circular pier model (CP) with collars two times the pier diameter (CPC-2) and circular pier model (CP) with outperformed the collars three times the pier diameter (CPC-3), offering the most significant reduction in scour depth. Using collars three times the pier diameter proved to be a promising approach to enhance the stability of circular piers and minimize scouring effects.

In the second case, when use nosed pier modal NP, nosed pier with airfoil-shaped collar (NPC-2) and nosed pier model with airfoil-shaped collar (NPC-3) are the results of three models. The NP model exhibited a maximum scour depth of 4.8 cm, and when fitted with airfoil-shaped collar (NPC-2), the scour depth reduced to 4 cm, resulting in an 18.4% reduction compared to the NP. On the other hand, the airfoil-shaped collar (NPC-3) model also achieved a maximum scour depth of 4 cm, showing a more significant reduction of 43.8% compared to the NP As shown in Figure.23.

In the second case, the results emphasize the significant improvement achieved by adding collars to the NP pier model. Both the (NPC-2) and (NPC-3) models displayed remarkable reductions in scour depth, outperforming the NP model without collars. The nosed pier model with airfoil-shaped collar (NPC-3) demonstrated greater efficacy in mitigating scouring around the pier compared nosed pier model with airfoil-shaped collar (NPC-2).

4.6.1 Comparison Between Circular Pier and Nosed Pier Model.

The comparison between the (CP) (circular pier without collar) and the NP model highlights the superior performance of the Downstream-facing round-nosed pier in reducing scour depth. The NP without airfoil-shaped collar achieved a 53.3% reduction in scour depth compared to the (CP). This indicates the advantage of utilizing Downstream-facing round-nosed piers in bridge design to enhance scour resistance and promote long-term stability as shown in Figure.23

4.6.2 Comparison Between (CP) with (NPC-2), (NPC-3), (CPC-2), (CPC-3).

Upon implementation of airfoil-shaped collars within the (NPC-2) and (NPC-3) models, which were attached to the nosed pier, when comparing it with results of the scour depth observed around the circular pier (CP), significant impacts were observed on the reduction in scour depth around the bridge pier. A significant decrease of approximately 61.2% happened within the (NPC-2) model, while an even more substantial extreme reduction of about 73.8% was realized within the (NPC-3) model. These reductions, as displayed in Figure 4.23. These findings highlight the pronounced efficacy of airfoil-shaped collars, particularly within the context of the (NPC-2) and (NPC-3) models attached to the nosed pier, in scour depth around bridge piers. This effect demonstrates as a notably higher reduction in scour around the bridge pier, in comparison to the impact of a circular pier with a circular collar in the (CPC-2) and (CPC-3) models as illustrated in Figures 4. 23 and 4. 24.

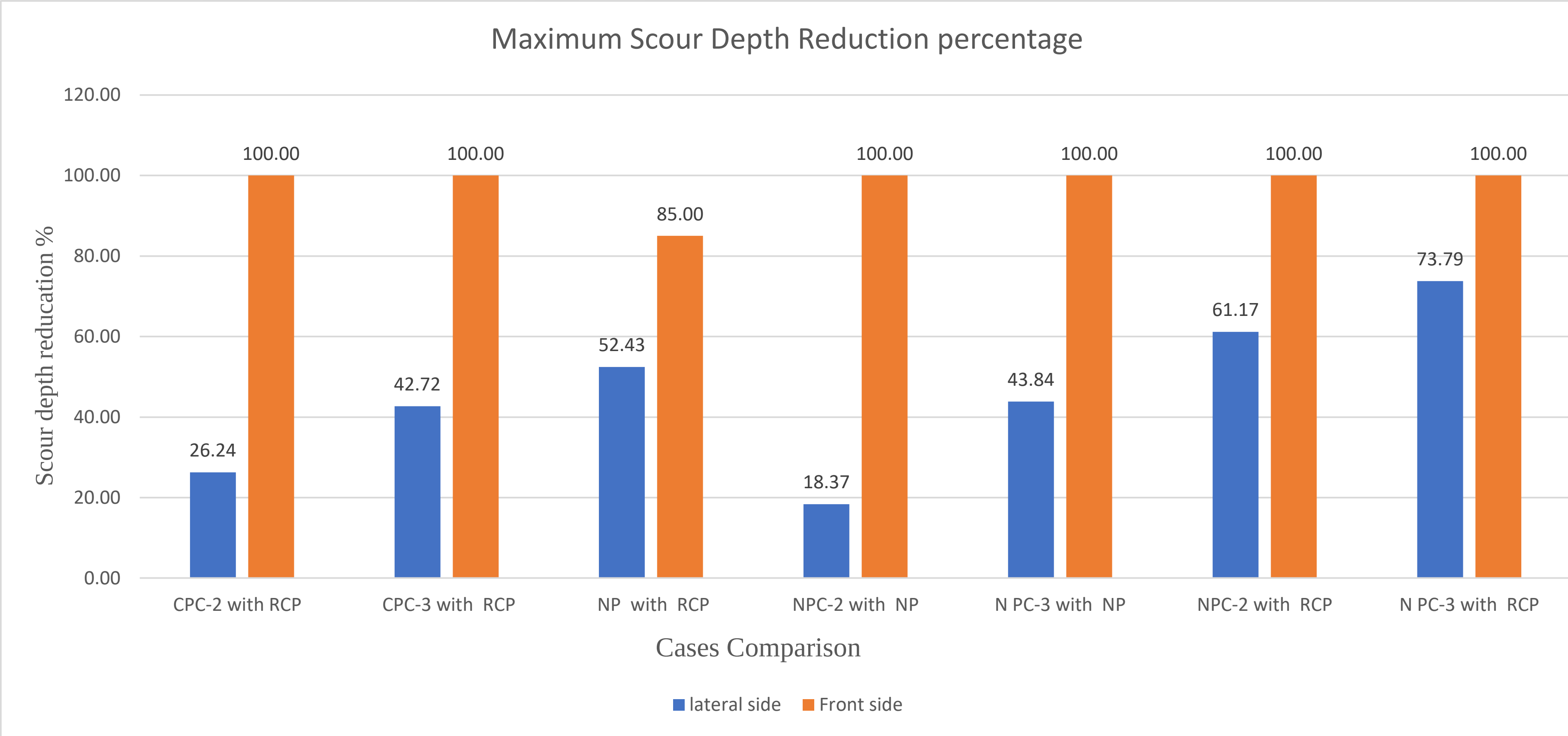

Figure 4.23 Results of reduction percentage in maximum Scour Depth.

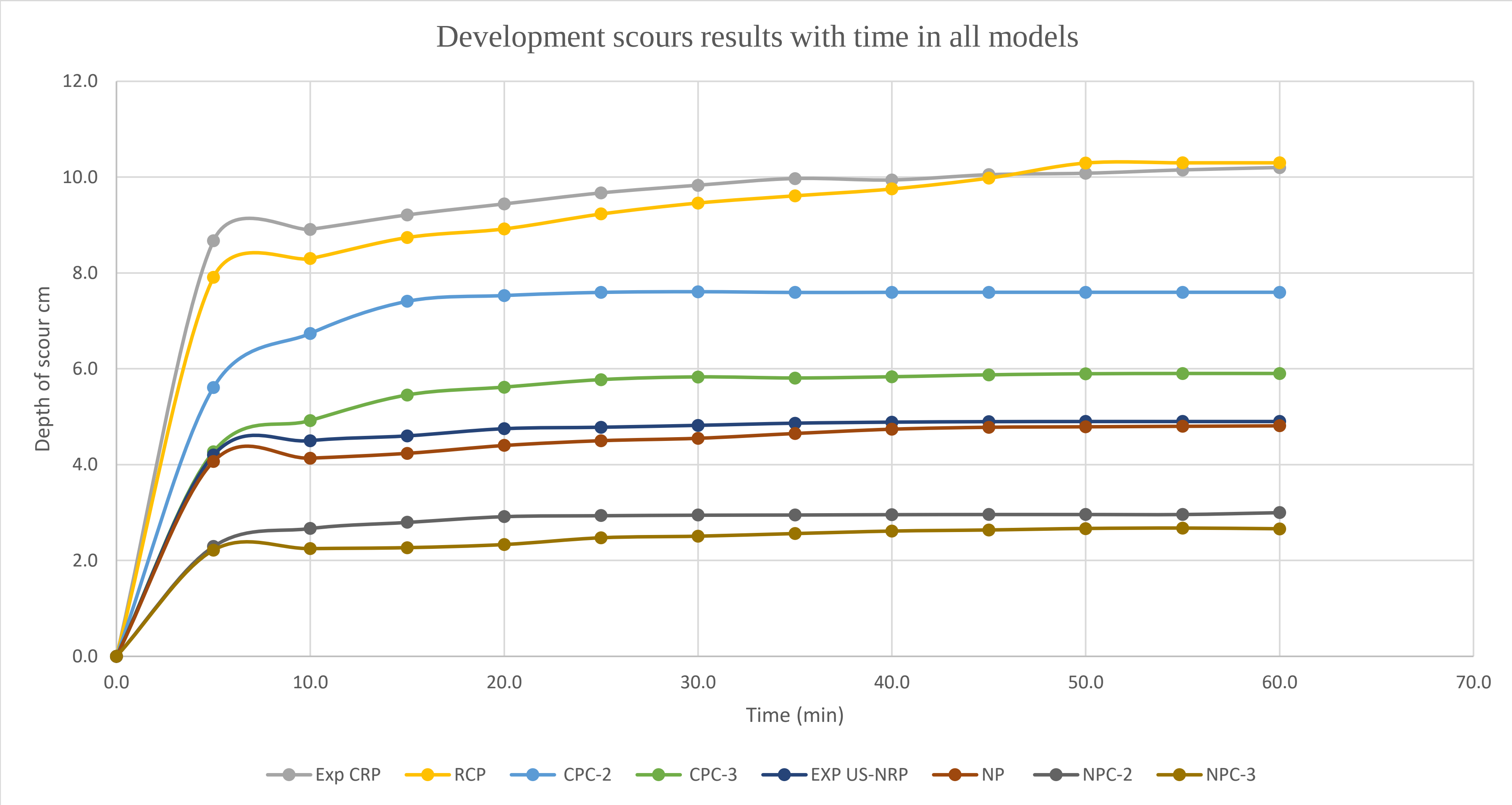

Figure 4.24 Development scours results with time in all models.

Table 4.1 Results of maximum depth of scouring for physical and numerical models with all cases.

Depth Of Scour										
Time (min)	**Discharge m^3/s**	**Flow Depth cm**	**Circular Pier**				**Nosied Pier**			
			Exp (CP)	**(CP)**	**CP-2**	**CP-3**	**Exp NP**	**NP**	**NPC-2**	**NPC-3**
0.00	0.058	12.50	0.00	0.00	0.00	0.00	0.00	0.00	0.00	0.00
5.00			8.67	7.91	5.61	4.27	4.20	4.07	2.29	2.22
10.00			8.91	8.30	6.74	4.92	4.50	4.14	2.67	2.25
15.00			9.21	8.74	7.41	5.45	4.60	4.24	2.80	2.27
20.00			9.44	8.92	7.53	5.62	4.75	4.40	2.92	2.33
25.00			9.67	9.23	7.60	5.77	4.78	4.50	2.94	2.47
30.00			9.83	9.46	7.61	5.83	4.82	4.55	2.95	2.51
35.00			9.97	9.61	7.59	5.81	4.87	4.65	2.95	2.56
40.00			9.94	9.75	7.60	5.83	4.89	4.74	2.96	2.61
45.00			10.05	9.98	7.60	5.87	4.90	4.78	2.96	2.64
50.00			10.08	10.30	7.60	5.89	4.90	4.79	2.96	2.67
55.00			10.15	10.30	7.60	5.90	4.90	4.80	2.96	2.68
60.00			10.20	10.30	7.60	5.90	4.90	4.81	3.00	2.66

CHAPTER 5
CONCLUSION AND RECOMMENDATION

5.1 Conclusion:

In this study, we investigated of flow and scour phenomena around two types of bridge piers: circular CP piers and nosed piers NP. The main focus was on evaluating the effectiveness of collar attachments in mitigating scouring effects and enhancing the stability of bridge piers. Through advanced numerical simulations using Flow-3D software, we gained valuable insights into the hydraulic forces and scour patterns around these pier models. The dynamics of horseshoe vortices and their impact on scour depth around bridge piers, whether circular or nosed, are influenced by various factors, including pier shape flow velocity, and turbulence.

5.1.2 First Case

The results from the first case demonstrated that the incorporation of collars significantly reduced scour depth around circular piers. Both the (CPC-2) and (CPC-3) models exhibited superior performance in comparison to the Reference Model CP without any collars. Notably, the (CPC-2) model, with collars at 3 times the pier diameter, yielded the most substantial scour depth reduction of 42.7%. These findings indicate that larger collars offer better protection and could be preferred in practical bridge design applications.

5.1.3 Second Case

In the second case, analyzed nosed piers model with and without airfoil-shaped collar attachments. the (NPC-2) and (NPC-3) model demonstrated remarkable reductions in scour depth, outperforming the nosed pier mode NP without collar. The results indicated that the use of collars, especially in (NPC-3) model, proved to be highly effective in minimizing scouring nosed piers model NP. This emphasizes the significance of incorporating collar countermeasures in bridge pier design, especially when dealing with Downstream-facing round-nosed piers. A noticeable decrease of the

(NPC-2) models, while an even more notable and substantial was achieved within the (NPC-3) model.

5.1.4 Overall Conclusion

Overall, this study highlights the importance of considering scouring effects during the design stage of bridge piers. Collar attachments prove to be an efficient and practical countermeasure in reducing scour depth and enhancing the stability of bridge foundations. A marked decrease of approximately 61.2% occurred within the (NPC-2) model, while an even more notable and substantial reduction of about 73.8% was achieved within the (NPC-3) model.

- These findings notably underscore the pronounced efficacy of airfoil-shaped collars, especially in the context of the (NPC-2) and (NPC-3) models affixed to the nosed pier, in mitigating the scour challenges surrounding bridge piers.
- This effectiveness becomes apparent as it results in a noticeably reduction in scour surrounding the bridge pier, compared to the impact of employing a circular pier with a circular collar as in the (CPC-2) and (CPC-3) models.
- The dynamics of horseshoe vortices and their impact on scour depth around bridge piers, whether circular or nosed, are influenced by various factors, including pier shape, flow velocity, and turbulence.
- Circular piers tend to generate more symmetrical and uniform horseshoe vortices due to their uniform shape. In contrast, nosed piers with tapered fronts exhibit distinct vortex patterns influenced by the gradual increase in pier width, leading to more complex flow dynamics and less scour depth.

5.2 Recommendations for Further research

Further research and experimentation should be conducted to explore the long-term performance and durability of collars under various flow conditions and sediment types. Additionally, investigating the potential impact of collars on the local ecology and riverbed dynamics could offer valuable insights.

To validate the effectiveness of collar countermeasures, it is recommended to carry out field tests on bridge piers in real-world cases. Field validation will provide practical data to supplement and validate the findings of numerical simulations.

To mitigate the adverse effects of scouring, such as erosion and structural instability, engineers have to take benefit from developing solutions. These collars are particularly effective when attached to circular bridge piers. They work by altering flow patterns, disrupting vortex formation, and diverting and dissipating water energy. This helps reduce vortex strings and scour depth, thereby enhancing the safety and longevity of bridge structures.

The results of this study underscore the importance of implementing countermeasures such as collars to mitigate scouring around bridge piers. By considering these recommendations in future bridge design and construction projects, engineers can improve the safety, resilience, and longevity of bridge structures, safeguarding critical infrastructure and enhancing overall sustainability.

References

Abusbeaa, A. M. (1986). Maximum scour around cylinders induced by wave and current action (Doctoral dissertation, University of British Columbia).

Akib, S., Jahangirzadeh, A., & Basser, H. (2014). Local scour around complex pier groups and combined piles at semi-integral bridge. Journal of Hydrology and Hydromechanics, 62(2), 108.

Alabi, P. D. (2006). Time development of local scour at a bridge pier fitted with a collar (Doctoral dissertation).

Barbhuiya, A. K., & Dey, S. (2004). Local scour at abutments: A review. Sadhana, 29, 449-476.

Bozkus, Z., & Yildiz, O. (2004). Effects of inclination of bridge piers on scouring depth. Journal of Hydraulic Engineering, 130(8), 827-832.

Breusers, H. N. C. (1965). Scouring around drilling platforms. J. Hydraul Res. IAHR, Bull., 19, 276.

Breusers, H. N. C., Nicollet, G., & Shen, H. W. (1977). Local scour around circular piers. Journal of hydraulic research, 15(3), 211-252.

Breusers, H. N. C., Nicollet, G., & Shen, H. W. (1977). Local scour around circular piers. Journal of hydraulic research, 15(3), 211-252.

Briaud, J. L., Chen, H. C., Li, Y., Nurtjahyo, P., & Wang, J. (2005). SRICOS-EFA method for contraction scour in fine-grained soils. Journal of geotechnical and geoenvironmental engineering, 131(10), 1283-1294.

Brownlie, W. R. (1983). Flow depth in sand-bed channels. Journal of Hydraulic Engineering, 109(7), 959-990

Chang, H. (1992). Fluvial Processes in River Engineering. Krieger Publishing Company, Florida, 432p.

Chiew, Y. M., (1992), Scour protection at bridge piers, Journal of Hydraulic Engineering, ASCE, Vol. 118, No. 11, pp. 1260–1269.

Chiew, Y. M., and Lim F. H. (2000). Failure behavior of riprap layer at bridge piers under live-bed conditions. Journal Hydraulic Engineering, ASCE, Vol. 126, No. 1, pp. 43–55.

Chiew, Y. M., and Lim F. H. (2000). Failure behavior of riprap layer at bridge piers under live-bed conditions. Journal Hydraulic Engineering, ASCE, Vol. 126, No. 1, pp. 43–55.

Cook, W. (2014). Bridge failure rates, consequences, and predictive trends. Utah State University.

Cook, W. (2014). Bridge failure rates, consequences, and predictive trends. Utah State University.

Dey, S. and Rajkumar V. R., (2007). Clear-water scour at piers in sand beds with an armor layer of gravels. Journal of Hydraulic Engineering, ASCE, Vol. 133, No. 6, pp. 703–711.

Ettema, R. (1980). Scour at bridge piers.

Ferraro, D., Tafarojnoruz, A., Gaudio, R., & Cardoso, A. H. (2013). Effects of pile cap thickness on the maximum scour depth at a complex pier. Journal of Hydraulic Engineering, 139(5), 482-491.

Froehlich, D. C. (1989). Local scour at bridge abutments. In Proceedings of the 1989 national conference on hydraulic engineering (pp. 13-18).

Gaudio, R., Grimaldi, C., Tafarojnoruz, A., & Calomino, F. (2010, May). Comparison of formulae for the prediction of scour depth at piers. In Proc., 1st IAHR European Division Congress (pp. 4-6). Edinburgh, UK: Heriot-Watt University.

Graf, W. H. (1984). Hydraulics of sediment transport. Water Resources Publication.

Gris, R. B. (2010). Sheath for reducing local scour in bridge piers. In Scour and Erosion (pp. 987-996).

Hamidi, A., & Siadatmousavi, S. M. (2018). Numerical simulation of scour and flow field for different arrangements of two piers using SSIIM model. Ain Shams Engineering Journal, 9(4), 2415-2426.

Hamill, L. (1998). Bridge hydraulics. CRC Press.

Hunt, B. E. (2005). Scour monitoring programs for bridge health. Transportation Research Record: Journal of the Transportation Research Board, (CD 11-S).

Ismael, A., Gunal, M., & Hussein, H. (2015). Effect of bridge pier position on scour reduction according to flow direction. Arabian Journal for Science and Engineering, 40, 1579-1590.

Kandasamy, J. K. (1989). Abutment scour. University of Auckland, School of Engineering Report, (458).

Kirwan, G., Demirci, B., Welch, H., Boyla, K., Özen, M., Castell, P., & Marlow, T. (2010). The birds of Turkey. Bloomsbury Publishing.

Kummar V., Ranga Raju K. G. and Vittal N., (1999). Reduction of local scour around bridge piers using slot and collar. Journal of Hydraulic Engineering, Vol. 125, No. 12, pp. 1302–1305.

Lagasse, P. F., & Richardson, E. V. (2001). ASCE compendium of stream stability and bridge scour papers. Journal of Hydraulic Engineering, 127(7), 531-533.

Lagasse, P., Zevenbergen, L., Schall, J. and Clopper, P., (2001). Bridge scour and stream instability countermeasures: Experience, selection, and design guidelines. FHWA NHI 01-003: Federal Highway Administration, Hydraulic Engineering Circular No. 23, 2nd ed., U.S. Department of Transportation, Washington, D.C

Lins, H. F. (2012). USGS hydro-climatic data network 2009 (HCDN-2009). US Geological Survey fact sheet, 3047(4).

Mashair, M. B., Zarrati, A. R., & Rezayi, A. R. (2004). Time development of scouring around a bridge pier protected by collar. In 2nd International Conference on Scour and Erosion, ICSE-2, Singapore (Vol. 8).

Melville, B. and Coleman, S., (2000). Bridge Scour. Water Resources Publications, LLC, Highlands Ranch, Colorado,

Melville, B.W., Chiew, Y.M., (1999). Time scale for local scour at bridge piers. J. Hydraul. Eng. ASCE 125 (1), 59–65.

Moody, J. A., Smith, J. D. and Ragan, B. W., (2005). Critical shear stress for erosion of cohesive soils subjected to temperatures typical of wildfires, Journal of Geophysical Research: Earth Surface, 110 (F1).

Muzzammil, M., Gangadharaiah, T., & Gupta, A. K. (2004, June). An experimental investigation of a horseshoe vortex induced by a bridge pier. In Proceedings of the institution of civil engineers-water management (Vol. 157, No. 2, pp. 109-119). Thomas Telford Ltd.

Ozalp, M. (2013). Experimental investigation of local scour around bridge pier groups. MSc Thesis. Middle East Technical University, Cankaya Ankara, Turkey.

Peck, R. B. Soil mechanics in engineering practice-K. Terzaghi EtAl-1966.

Rajaratnam, N., & Nwachukwu, B. A. (1983). Erosion near groyne-like structures. Journal of hydraulic Research, 21(4), 277-287.

Robert, E., Tatsuaki, N., and Marian M., (2006). an illustrated guide for monitoring and protecting bridge waterways against scour, Iowa Highway Research Board, Project TR-515 Final Report, IIHR Technical Report No. 449.

Shahriyar, M. A. (2021). Numerical investigation of local scour around different shaped bridge piers using flow 3d software (Doctoral dissertation, Department of Mechanical and Production Engineering (MPE), Islamic University of Technology (IUT), Board Bazar, Gazipur, Bangladesh).

Shan, H., Kilgore, R., Shen, J., & Kerenyi, K. (2016). Updating HEC-18 pier scour equations for noncohesive soils (No. FHWA-HRT-16-045). United States. Federal Highway Administration. Office of Infrastructure Research and Development.

Sheppard, D. M., Odeh, M., & Glasser, T. (2004). Large scale clear-water local pier scours experiments. Journal of Hydraulic Engineering, 130(10), 957-96

Shirhole, A. M., & Holt, R. C. (1991). Planning for a comprehensive bridge safety program. Transportation Research Record, 1290, 39-50.

Su, C. C., & Lu, J. Y. (2013). Measurements and prediction of typhoon-induced short-term general scours in intermittent rivers. Natural hazards, 66, 671-687.

Tafarojnoruz, A., Gaudio, R., & Dey, S. (2010). Flow-altering countermeasures against scour at bridge piers: a review. Journal of hydraulic research, 48(4), 441-452.

Tey, C. B., Raudkivi, A. J., & Melville, B. W. (1984). Local Scour at Bridge Abutments: A Report Submitted to the Roard [ie Road] Research Unit of the National Roads Board. Department of Civil Engineering, University of Auckland.

Tison, L. J. (1961). Local scour in rivers. Journal of Geophysical Research, 66(12), 4227-4232.

Tulimilli, B. R., Majumdar, P. and KOSTIC M., (2003). Development of CFD Simulation for 3-D Flooding Flow and Scouring Around a Bridge Structure, Argonne National Laboratory West Chicago, IL U.S.A

Wardhana, K., & Hadipriono, F. C. (2003). Analysis of recent bridge failures in the United States. Journal of performance of constructed facilities, 17(3), 144-150.

Whitehouse, R. J., & Harris, J. (2014). Scour prediction offshore and soil erosion testing.

Yanmaz, A. M., Altinbilek, H. D., (1991). Study of Time-Dependent Local Scour around Bridge Piers, J. Hydraulic Engineering. Vol. 117, No.10,1247-1268.

Yanmaz, A., (2002). Dynamic reliability in bridge pier scouring. Turkish Journal of Engineering and Environmental Sciences, 26, 367-375.

Zevenbergen, L. W. (2010). Comparison of the HEC-18, Melville, and Sheppard Pier Scour Equations. In Scour and Erosion (pp. 1074-1081).

CURRICULUM VITAE

Yousef Alhammoudi

EDUCATION

2012-2023 Master Degree in Civil Engineering, Gaziantep University, Gaziantep, Türkiye.

1993-1998 B.Se in Civil Engineering, Aleppo University, Aleppo, Syria.